

Impact of Flashover Fire Conditions on Exposed Energized Electrical Cords and Cables

Craig Weinschenk
Daniel Madrzykowski
Paul Courtney*

UL Firefighter Safety Research Institute
Columbia, MD 21045

*UL LLC
Northbrook, IL 60062



Impact of Flashover Fire Conditions on Exposed Energized Electrical Cords and Cables

Craig Weinschenk
Daniel Madrzykowski
Paul Courtney *

UL Firefighter Safety Research Institute
Columbia, MD 21045

*UL LLC
Northbrook, IL 60062

Revised October 2, 2019



UL Firefighter Safety Research Institute
Stephen Kerber, Director

In no event shall UL be responsible to anyone for whatever use or non-use is made of the information contained in this Report and in no event shall UL, its employees, or its agents incur any obligation or liability for damages including, but not limited to, consequential damage arising out of or in connection with the use or inability to use the information contained in this Report. Information conveyed by this Report applies only to the specimens actually involved in these tests. UL has not established a factory Follow-Up Service Program to determine the conformance of subsequently produced material, nor has any provision been made to apply any registered mark of UL to such material. The issuance of this Report in no way implies Listing, Classification or Recognition by UL and does not authorize the use of UL Listing, Classification or Recognition Marks or other reference to UL on or in connection with the product or system.

NOTE: This report was originally published on April 11, 2019 and subsequently submitted for publication in *Fire Technology*. During the assessment process, the reviewers made several recommendations to strengthen the report for publication. Where appropriate, those edits have been incorporated into the revised version of this report.

Contents

List of Figures	ii
List of Tables	iii
1 Background	2
2 Objectives	5
2.1 Notes on the Study	5
3 Experimental Configuration	6
3.1 Experimental Room	6
3.2 Instrumentation	7
3.3 Fuel Load	9
3.4 Electrical Test Configuration	11
3.5 Test Procedure	15
4 Results	16
4.1 Thermal Exposure	16
4.2 Electrical Response	21
5 Discussion	26
5.1 Heat Flux Analysis	26
5.2 Physical Inspection of Cords	27
6 Future Research Needs	32
7 Summary	33
References	34
A Available Fault Current	36
B Gain Calculations	37
C Fault Data	38
D Physical Cord Damage	42

List of Figures

3.1	Overall Dimensions of the Test Room	7
3.2	Test Fixture Instrumentation	8
3.3	Dimensioned Fuel Layout	10
3.4	Heat Release Rate of Sofas	11
3.5	Schematic of Electrical Test Setup	12
3.6	Photograph of Installed Cords/Cables	15
4.1	Heat Release Rate of Experiments	16
4.2	Photographs of Test Room During Flashover	17
4.3	Mid-Room Thermocouple Temperatures	18
4.4	Experiments 5 and 6 – Heat Flux	19
4.5	Experiment 1 – Ceiling Debris	20
4.6	Experiment 1 – Heat Flux	20
4.7	Experiment 1 – Signal Data of Thermal Magnetic Breaker with 18-2 SPT1 Cord	21
4.8	Experiment 1 – Signal Data of GFCI Breaker with 12-2 NM-B Cable	22
4.9	Experiment 5 – Signal Data of AFCI Breaker with 12-2 NM-B Cord	23
4.10	Experiment 6 – Signal Data of AFCI Breaker with 16-3 SJTW Cord	24
5.1	Photograph of Cords Following Experiment	27
5.2	Magnified Photograph of 12-2 NM-B Cable Following Experiment 2	28
5.3	Magnified Post Experiment Photograph of 16-3 SJTW Cord with Thermal Magnetic Circuit Breaker	29
5.4	Magnified Post Experiment Photograph of 16-3 SJTW Cord with AFCI	29
5.5	Magnified Post Experiment Photograph of 16-3 SJTW Cord with GFCI	30

List of Tables

3.1	Electrical Fault Testing Experiments Fuel Load	9
3.2	Description of Furnishing and Interior Finish Fuel Package	9
3.3	Sofa HRR Data	11
3.4	Electrical Fault Test Setup	14
3.5	Description of Cord/Cable Types	14
4.1	HRR, Total Energy, and Trip Times from Room Experiments	17
4.2	Circuit Trip Type for Each Experiment	25
5.1	Mean and Standard Deviation of Integrated Heat Flux for Each Cord Type at Trip	26
A.1	Available Fault Current Data	36
A.2	Fault Current Calculation Definitions	36
B.1	Gain Calculations	37
C.1	Circuit Trip Data for Experiment 1	38
C.2	Circuit Trip Data for Experiment 2	39
C.3	Circuit Trip Data for Experiment 3	39
C.4	Circuit Trip Data for Experiment 4	40
C.5	Circuit Trip Data for Experiment 5	40
C.6	Circuit Trip Data for Experiment 6	41
D.1	Post Experiment Physical Observations on Cords	42

List of Abbreviations

AFCI	Arc-fault circuit interrupter
GFCI	Ground-fault circuit interrupter
HRR	Heat release rate
MCCB	Molded case circuit breaker
MDF	Medium density fiberboard
NFPA	National Fire Protection Associations
NIJ	National Institute of Justice
NISPT	Non-integral service parallel thermoplastic
NM-B	Type B, non-metallic sheathed, thermoplastic insulated, more heat-resistant than older “NM” cable
SJTW	Thermoplastic hard jacket, water resistant
SPT	“Zip Cord”, thermoplastic insulation
SVT	Hard service cord, thermoplastic insulation
TC	Thermocouple
UL FSRI	UL Firefighter Safety Research Institute

Acknowledgments

This project was supported by Award No. 2015-DN-BX-K052, awarded by the National Institute of Justice, Office of Justice Programs, U.S. Department of Justice. The opinions, findings, and conclusions or recommendations expressed in this publication/program/exhibition are those of the author(s) and do not necessarily reflect those of the Department of Justice.

To assist in the design and implementation of the experiments for this study, fire service experts with knowledge in fire investigation and burn patterns were gathered from across the United States. The individuals below provided direction for the project by assisting in planning the experiments, witnessing the testing, and developing concrete conclusions. Their tireless support and efforts make this project relevant to the fire safety community across the world.

Fire Investigation Technical Panel

Name	Affiliation
Robert Byrnes	Fire Department City of New York (ret.)
Steve Carman	Carman & Associates Fire Investigation, Inc
Paul Claffin	Bureau of ATF, Fire Investigation & Arson Enforcement Division
Chris Connealy	Texas State Fire Marshal, TDI Deputy Insurance Commissioner
Richard Dyer	Dyer Fire Consulting
John Golder	Forensic Investigation and Consultation, LLC
Mark Goodson	Goodson Engineering
David Icove	University of Tennessee, Knoxville
Thomas Kane	Fire Department City of New York
John Lentini	Scientific Fire Analysis, LLC
Thomas Lichtenstein	UL LLC
Jeffrey Lyle	Chicago Fire Department
Kevin McGrattan	National Institute of Standards and Technology
Robert Pyzyna	Northbrook Fire Department

The authors would also like to acknowledge Paul Brazis, Kelly Opert, Robert James, and the technical staff from the large fire lab of UL LLC for their dedication in conducting these full-scale experiments. These experiments would not have been possible without the UL FSRI team. The UL FSRI team instrumented, conducted, and analyzed these experiments. The authors thank: Robin Zevotek, Keith Stakes, Jack Regan, Joshua Crandall, Steve Kerber, Sarah Huffman, and especially Roy McLane of Thermal Fabrications.

Executive Summary

A set of experiments was conducted to expose different types of energized electrical cords for lamps, office equipment, and appliances to a developing room fire exposure. All of the cords were positioned on the floor and arranged in a manner to receive a similar thermal exposure. Six types of cords commonly used as power supply cords, extension cords, and as part of residential electrical wiring systems were chosen for the experiments. The non-metallic sheathed cables (NM-B) typically found in residential electrical branch wiring were included to provide a link to previous research. The basic test design was to expose the six different types of cords, on the floor of a compartment to a growing fire to determine the conditions under which the cord would trip the circuit breaker and/or undergo an arc fault. All of the cords would be energized and installed on a non-combustible surface.

Six cord types (18-2 SPT1, 16-3 SJTW, 12-2 NM-B, 12-3 NM-B, 18-3 SVT, 18-2 NISPT-2) and three types of circuit protection (Molded case circuit breaker (MCCB), combination Arc-fault circuit interrupter (AFCI), Ground-fault circuit interrupter (GFCI)) were exposed to six room-scale fires. The circuit protection was remote from the thermal exposure. The six room fires consisted of three replicate fires with two sofas as the main fuel source, two replicate fires with one sofa as the main fuel source and one fire with two sofas and MDF paneling on three walls in the room. Each fuel package was sufficient to support flashover conditions in the room and as a result, the impact on the cords and circuit protection was not significantly different. The average peak heat release rate of the sofa fueled compartment fires with gypsum board ceiling and walls was 6.8 MW. The addition of vinyl covered MDF wall paneling on three of the compartment walls increased the peak heat release rate to 12 MW, although most of the increased energy release occurred outside of the compartment opening. In each experiment during post flashover exposure, the insulation on the cords ignited and burned through, exposing bare conductor. During this period the circuits faulted.

The circuit protection devices are not designed to provide thermal protection, and, thus, were installed remote from the fire. The devices operated as designed in all experiments. All of the circuit faults resulted in either a magnetic trip of the conventional circuit breaker or a ground-fault trip in the GFCI or AFCI capable circuit protection devices. Though not required by UL 1699, *Standard for Safety for Arc-Fault Circuit-Interrupters* as the solution for detection methodology, the AFCIs used had differential current detection. Examination of signal data showed that the only cord types that tripped with a fault to ground were the insulated conductors in non-metallic sheathed cables (12-2 NM-B and 12-3 NM-B). This was expected due to the bare grounding conductor present.

Assessments of both the thermal exposure and physical damage to the cords did not reveal any correlation between the thermal exposure, cord damage, and trip type.

1 Background

According to NFPA 921, *Guide for Fire and Explosion Investigation*, there are four types of analysis that may be conducted to determine the area of origin of a fire: witness information, fire patterns, arc mapping, and fire dynamics [1]. In 2014, the Fire and Arson Investigation Technology Working Group Operational Requirements issued a set of operational requirements that included the characterization of electrical system response to fire as a research need [2].

These two documents motivate the current study. Fire investigators often find the remains of power cords that have been exposed to fire. The technical panel members agreed that there are two topics of interest: the thermal exposure of the cord prior to circuit trip, and the arc damage to cords following the trip of a circuit breaker.

As defined by NFPA 921, an arc fault involves a high-temperature, luminous electric discharge across a gap or through a medium such as charred insulation [1]. More specifically, arcing will occur between conductive surfaces once the insulation carbonizes, as carbon is a narrow bandgap semiconductor and can facilitate initiation of an arcing condition. Further, fire is electrically conductive and has the potential to short circuit electrified surfaces.

Béland developed several articles on the topic of arcing in the early 1980s [3–5]. Béland states that when energized electric wiring, such as power cords, from fixtures or appliances, or extension cords, were exposed to a fire environment, arcing was likely to occur due to the thermal degradation of the cord’s insulation. One of the articles provided a few rough estimates of time to arcing. For a fire “well in progress” the time to arcing of the cord would be approximately one minute for extension cords, three minutes for plastic sheathed cables, five minutes for a braided non-metallic sheathed cable and around ten minutes for cords in metallic conduit [5].

Safety Engineering Laboratories, Inc. conducted a bench-scale study which exposed energized two conductor power cords, the type used for televisions and electronic appliances, to an electric radiant heat source with a flux of 40 kW/m^2 [6] with an exposure duration that did not exceed 15 minutes. Damage to the copper cords ranged from localized fusing to severed cords. The energized cords did not always leave evidence of electrical arcs after the radiant thermal exposure. However, energized cords that were in contact with combustible surfaces or that were ignited by the radiant exposure, always provided evidence of electrical faults. Further the study did not find any correlations between the arc damage and the fire exposure, the type and construction of the insulating material, and magnitude or duration of the fault current. The time to the electrical fault occurred between approximately four and seven minutes. Additional cords were exposed to an open flame. In these cases, the electrical faults occurred in three minutes or less.

Novak conducted an extensive study of NM-B 14-2 cables. The cable test samples had a 102 mm long section that was exposed to a nearly uniform heat flux. Energized and non-energized cords were exposed to heat fluxes ranging from 20 kW/m^2 to 55 kW/m^2 . The source of the heat flux was an electric heater element from a cone calorimeter. Novak found that ignitions of the cord

insulation generally occurred between 50 and 55 kW/m², minimum heat flux to cause a faulted circuit was 22 kW/m², and the time-to-failure of the cables was related to the heat flux exposure [7].

Many other studies have been conducted where NM type solid core electrical cords were installed on the ceilings and walls of compartments and exposed to fire environments. These experiments have focused more on the location of the damage to the cord for purposes of examining arc mapping, as opposed to examining the thermal conditions that generated the damage. Babrauskas has recently published a review of arc mapping which includes references to this body of work [8].

Another consideration was the type of circuit protection that should be used in the fire experiments. There are three basic types of circuit protection: 1) “conventional” circuit breaker (MCCB), 2) Ground-Fault Circuit Interrupter (GFCI), and 3) Arc-Fault Circuit Interrupter (AFCI). Each action or purpose of each type of circuit protection is provided by the National Electric Code [9] and is briefly described below.

The molded case circuit breaker (MCCB) is a device designed to open and close a circuit by nonautomatic means and to open the circuit automatically on a predetermined over-current without damage to itself when properly applied within its rating. The typical activation mechanism for a conventional circuit breaker is either a bi-metallic strip (thermal) or an electro-magnetic switch.

The GFCI is designed to de-energize a circuit when the supplied and returned current differ by more than 5 mA ± 1 mA for a Class A device. The differential current is assumed to be returning by some other pathway, which may be due to a ground fault condition. A ground fault is defined as “an unintentional, electrically conductive connection between an ungrounded conductor of an electrical circuit and the normally non-current-carrying conductors, metallic enclosures, metallic raceways, metallic equipment, or earth [9].”

The AFCI is intended to provide protection from the effects of arc faults. The AFCI monitors current waveforms and de-energizes the circuit when a waveform characteristic of an arc fault is detected. While not typical, AFCI devices may also be capable of performing other functions such as over-current protection, ground-fault circuit interruption, and surge suppression.

After reviewing the existing information and the technical panel input, a set of experiments was designed to expose different types of energized electrical cords to a developing room fire exposure. All of the cords would be positioned on the floor and arranged in a manner to receive a similar thermal exposure. The technical panel identified six types of cords commonly used in North American homes. All of the cords would be energized and they would be installed on a non-combustible surface. Non-metallic sheathed cables (i.e. Romex), typically found in residential electrical branch circuits, were included to provide a link to previous research. Note, the exposure of the non-metallic insulated cords on the floor is not representative of how it would typically be exposed in a real-world environment.

Further, the cords were connected to three different types of circuit protections. Therefore, the decision regarding the basic test design was made to expose the six different types of cords, positioned on the floor of a compartment, to a growing fire to determine when and under what conditions the local cord failures would cause the circuit protection devices to trip. It was not expected that any

of the circuits would detect cord ignition.

2 Objectives

The following objectives were developed for this study:

1. Determine if there are critical thermal exposure conditions to the cords.
2. Determine if the cord type affected the trip type when exposed to fire conditions.
3. Determine if the remote circuit protection type affected trip type when cords were exposed to fire conditions.
4. Determine if a correlation can be made between the cord damage and the trip type.

For these experiments, fire conditions were defined by a fuel load in a single compartment sufficient to sustain flashover within that compartment. In addition to the electrical fault related questions, the repeatability of the fire conditions, and the impact of changes to the fuel load within the fire room were examined.

2.1 Notes on the Study

In conducting the experiments detailed in this report, there are several key points that need to be highlighted to ensure there is appropriate context for this work.

- The circuit protective devices were located at a panel board on an external side wall of the fire compartment and not directly exposed to the same thermal conditions as the cords. In other words, the circuit breakers were unaffected by the fire throughout the test. Additionally an AFCI, by design, is not intended to detect burning of a cord nor glowing connections.
- These experiments were not designed to test the operating performance of circuit breakers. An example would be the electrical setup that is required for AFCIs in UL 1699. There was high available current in these experiments (approximately 750 A) and a short homerun distance (5.5 m (18 ft)). The results of these experiments may likely be different using 500 A available short circuit current and a 15.3 m (50 ft) home run .
- A typical installation of NM-B cable in a residential structure would be through a stud, behind gypsum board. The exposed NM-B cables thus had an atypical setup in these experiments, specifically to link to prior research.
- Similar to what could occur in a residential structure, there were two-conductor cords connected to both GFCI and ACFI circuits. In these cases, it was not expected that those circuits would behave differently than a conventional circuit.

3 Experimental Configuration

3.1 Experimental Room

A fire room with a single opening was constructed in Underwriters Laboratories' calorimetry laboratory in Northbrook, IL. The laboratory footprint is approximately 13.1 m (43.0 ft) by 14.6 m (48.0 ft). The calorimeter has the capacity to measure both chemical (oxygen consumption calorimetry) and convective (thermopile calorimetry) heat release rates. The diameter of the smoke collection exhaust hood is 7.6 m (25.0 ft), and it is positioned approximately 7.6 m (25.0 ft) from the floor.

The interior dimensions of the test room were 3.7 m (12.0 ft) by 3.7 m (12.0 ft) by 2.4 m (8.0 ft) tall. The only opening measured 2.4 m (8.0 ft) wide by 2.0 m (6.7 ft) high and was located on the front wall of the room. The walls and ceiling were lined with one layer of 1.6 cm (0.625 in.) thick type X gypsum board and one layer of 1.3 cm (0.5 in.) thick conventional gypsum board supported by 3.8 cm by 8.9 cm (2 in. by 4 in.) wood studs.

The floor was built with 3.8 cm by 15.2 cm (2 in. by 6 in.) wood joists covered with 1.3 cm (0.5 in.) thick plywood and 1.3 cm (0.5 in.) thick cement board. The front face of the room was covered with 1.3 cm (0.5 in.) cement board to prevent fire spread to the exterior of the compartment. Figure 3.1 shows the dimensions of the room in plan view. For the final experiment, the room was lined with decorative vinyl-laminated medium density fiberboard (MDF) paneling, 3.5 mm (0.14 in.) thick, with a density of 0.12 kg/m^3 on the four interior walls.

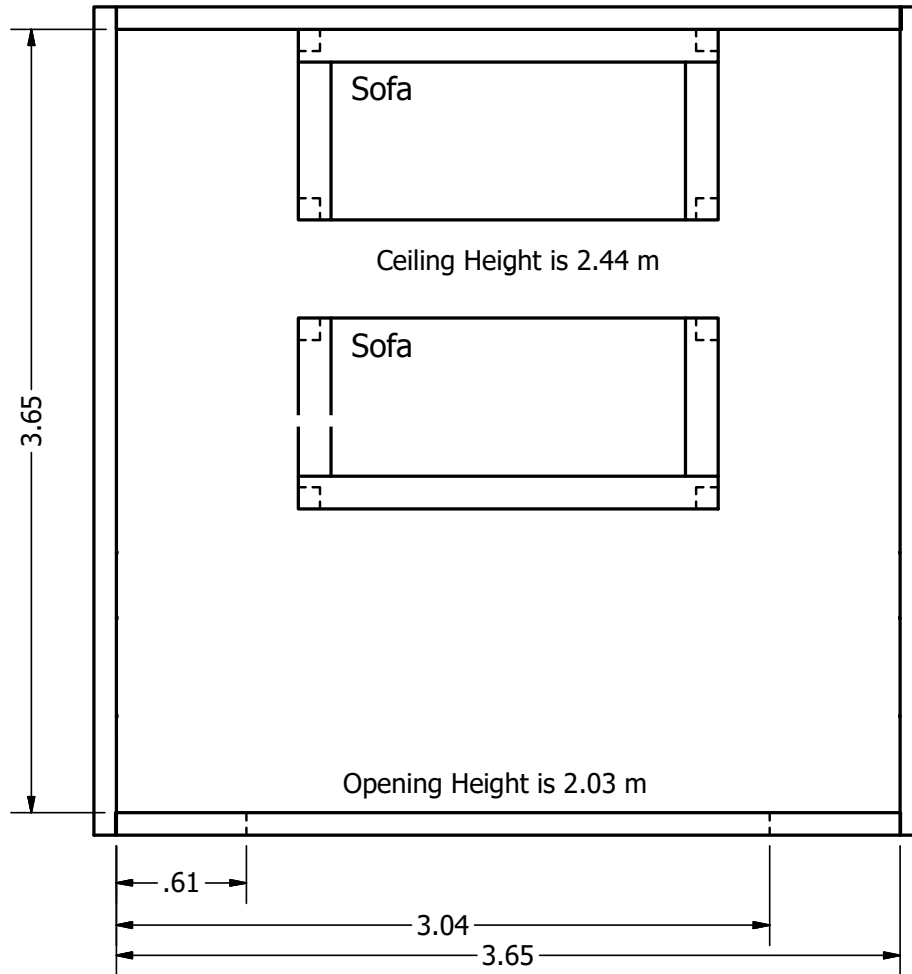


Figure 3.1: Major dimensions of test structure including the large opening size. Dimensions are in meters.

3.2 Instrumentation

Temperature and heat flux measurements were taken within the compartment to characterize the thermal environment. Gas temperatures were measured with 1.3 mm (0.05 in) diameter, bare-bead, Chromel-Alumel (type K) thermocouples while Schmidt-Boelter gauges were used to measure total heat flux. Results from an international study on total heat flux gauge calibration and response demonstrated that the uncertainty of a Schmidt-Boelter gauge is typically $\pm 8\%$ [10]. Two thermocouple arrays, with eight thermocouples per array, and nine heat flux gauges were installed in the room. Small diameter thermocouples were used to limit measurement uncertainty, which is estimated to be $\pm 15\%$ for these experiments [11, 12]. Figure 3.2 shows the spatial location of the instrumentation within the test room. The top thermocouple in each array was located 2.54 cm (1 in.) below the ceiling with the remaining 7 spaced at 30.5 cm (1 ft) intervals (30.5 cm below ceiling, 61 cm below ceiling ... 213 cm below ceiling). For more information regarding the cord exposures, see Section 3.4.

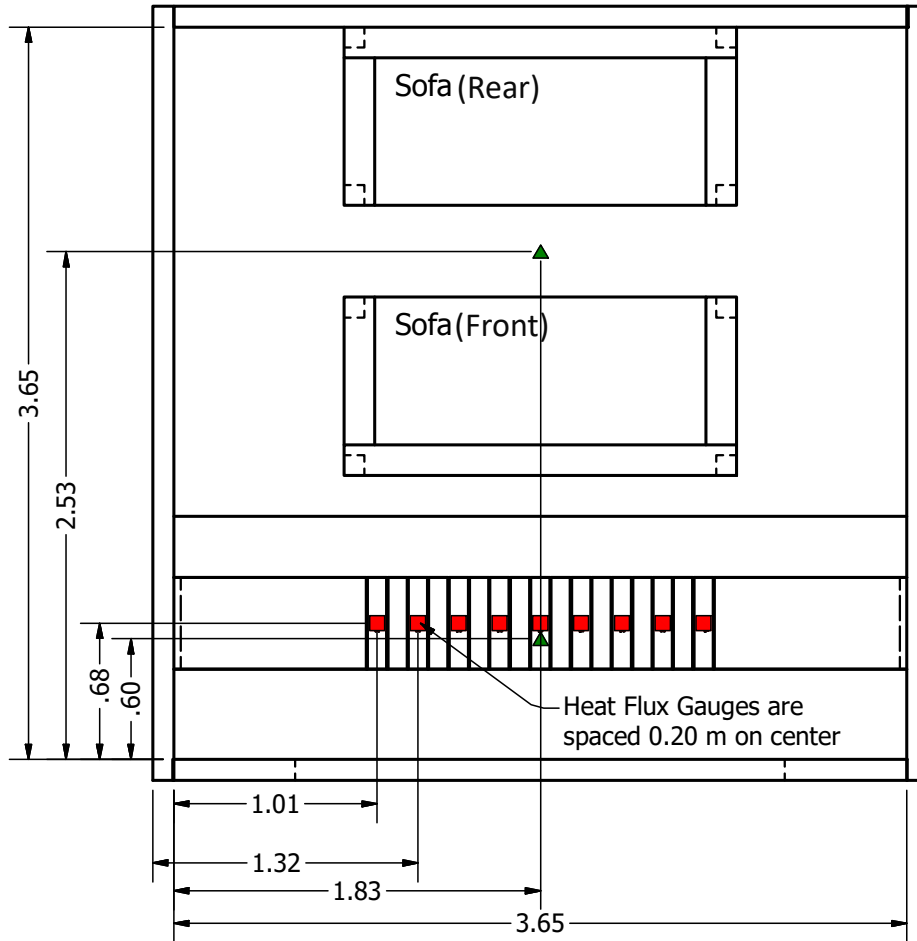


Figure 3.2: Dimensioned instrumentation configuration. Dimensions are in meters. Red squares are heat flux gauges and green triangles are thermocouple arrays.

In addition to the instrumentation in the test room, the laboratory was instrumented to capture heat release rate (HRR). The test room was oriented inside the lab such that combustion products produced from the experiments were collected by the 7.6 m (25 ft) diameter smoke collection exhaust hood. For these experiments oxygen consumption calorimetry was used [13]. To ensure capture of the smoke produced (i.e., quantify the drop in oxygen concentration from combustion products) during the experiments, the exhaust duct was operated at $14 \text{ m}^3/\text{s}$ (30,000 CFM). The heat release calorimeter has been calibrated with a steady fire size of approximately 10 MW from a heptane spray burner. Bryant and Mullholland [14] estimate the uncertainty of oxygen consumption calorimeters measuring high heat release rate fires at $\pm 11\%$.

3.3 Fuel Load

The primary fuel load, a three-seat sofa, was chosen to be representative of a residential living room. The wood-based sub-floor was covered with a 12.7 mm (0.5 in.) layer of polyurethane foam padding. The padding was covered with carpeting composed of Olefin fiber attached to a polypropylene backing material. In the sixth experiment, the walls were lined with 3.5 mm (0.14 in.) vinyl-covered MDF panels. In Experiments 4–5, only one sofa was used instead of two. Table 3.1 shows the fuel load for each of the experiments.

Table 3.1: Electrical Fault Testing Experiments Fuel Load

Exp #	Sofas	Flooring	Lining
1	2	Padding & Carpet	Gypsum
2	2	Padding & Carpet	Gypsum
3	2	Padding & Carpet	Gypsum
4	1	Padding & Carpet	Gypsum
5	1	Padding & Carpet	Gypsum
6	2	Padding & Carpet	MDF

The sofas were purchased new. The body and the cushions of the sofa were upholstered in 100 % polyester fabric. The seat cushions were filled with 127 mm (5 in) thick polyurethane foam pads, with a layer of 25 mm (1 in) polyester batting on the top and bottom of the polyurethane pads. The back cushions were filled with polyester batting. Table 3.2 provides detailed information regarding the composition and mass of the fuel used in the experiments.

Table 3.2: Description of Furnishing and Interior Finish Fuel Package

Item	Quantity	Material Description	Dimensions (m)	Mass (kg)	Total Mass (kg)
Sofa	2	Polyester fabric, batting, PUF	2.20 L by 0.91 D by 0.91 H	47.5	95.0
Carpet	8.9 m ²	100 % Olefin fiber w/PP backing	3.68 L by 6.05 W	33.0	33.0
Padding	8.9 m ²	PU foam	3.66 L by 2.44 W by 12.7 mm H	7.3	7.3
Sub-Floor	8.9 m ²	Oriented strand board	3.66 L by 2.44 W by 17.9 mm H	116.0	116.0
*Paneling	26.7 m ²	Medium density fiberboard	2.44 L by 1.22 W by 3.5 mm H	10	89.7
				Total Mass	341.0

* Paneling was only used in Experiment 6

Figure 3.3 shows a dimensioned layout of the fuel within the test structure for the two sofa configuration. The hatched area is the portion of the floor area covered by padding and carpet.

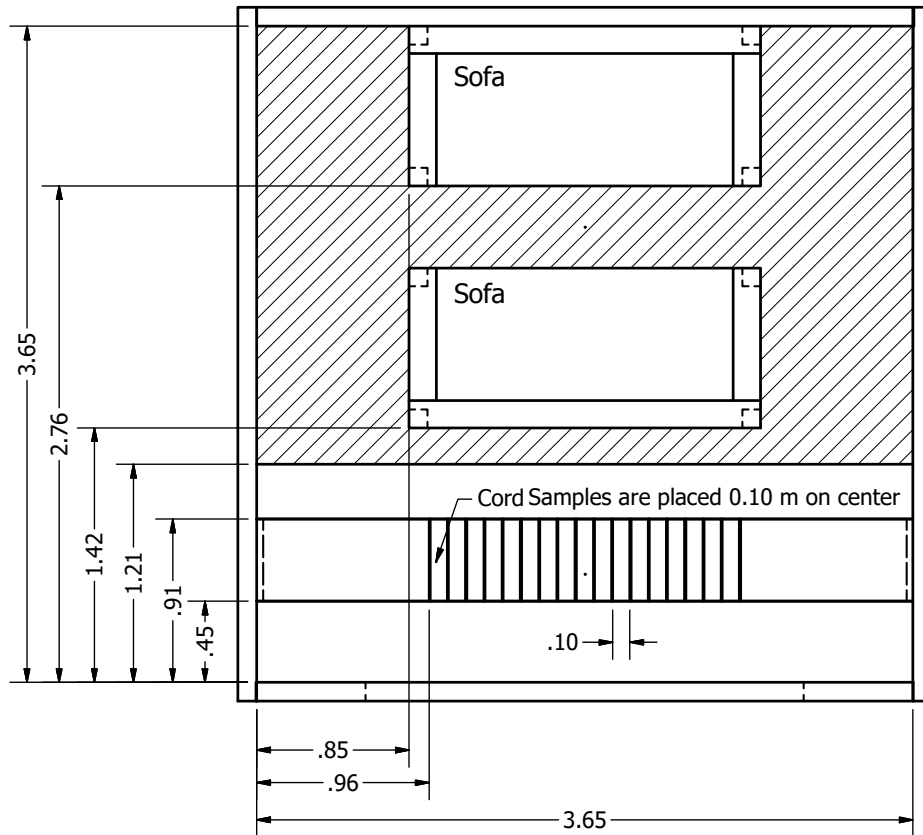


Figure 3.3: Two sofa furniture layout. In the test with one sofa, the sofa was positioned along the wall opposite the opening. The hatched area represents the area covered by carpet and padding. Dimensions are in meters.

To understand the magnitude and repeatability energy release of the primary fuel package used in these experiments, three sofas were ignited with an electric matchbook and burned in the absence of a compartment and quantified using oxygen consumption calorimetry. The heat release rate (HRR) as a function of time for the three sofas is included in Figure 3.4.

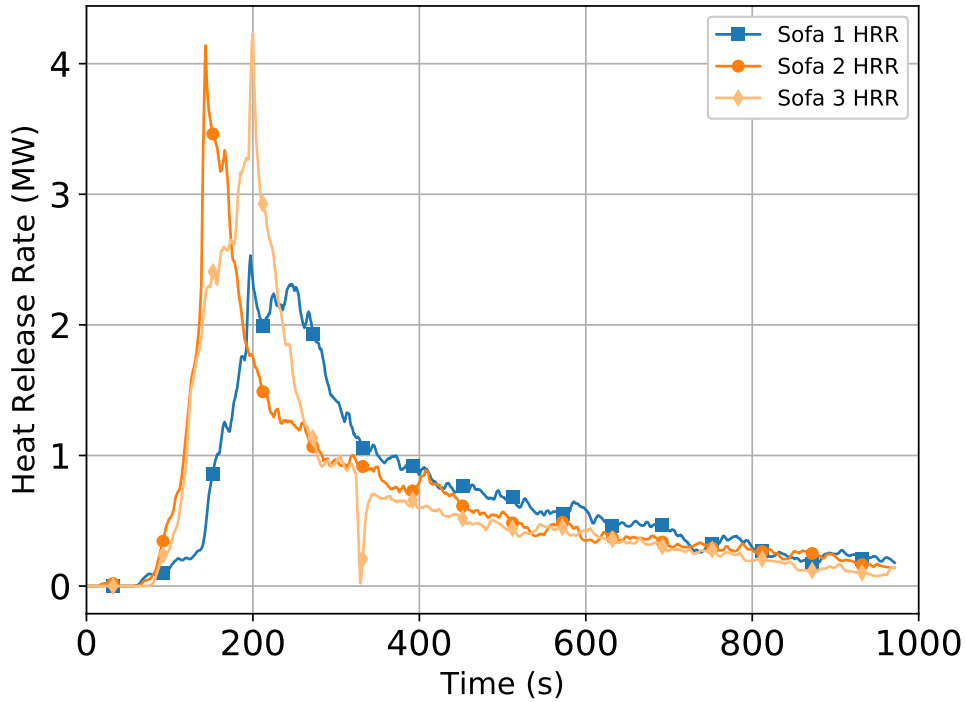


Figure 3.4: Heat release rate versus time replicates for sofas used in experiments.

Sofa 1 had a peak HRR of 2.5 MW while the peak HRR for sofa 2 and sofa 3 were 4.1 MW and 4.2 MW, respectively. The peak HRR for sofas 2 and 3 were within the typical uncertainty of the measurement. The peak HRR from sofa 1 was approximately 40% lower than the other two sofas, which highlights the natural variability of fuel. An integration over time for the HRR was conducted to calculate the total energy release. The total energy release showed similarity (10% difference) between all three sofas. Table 3.3 shows the peak HRR and total energy release for each sofa.

Table 3.3: Sofa HRR Data

Sofa #	Peak HRR (MW)	Total Energy Released (MJ)
1	2.5	655
2	4.1	649
3	4.2	639

3.4 Electrical Test Configuration

To ensure any concurrent experiments within the laboratory did not impact the electrical configuration for these experiments and to match the impedance of a typical residential home, the system

was powered by 120 kW/150 kVA, 3-phase AC generator. Figure 3.5 is a line drawing schematic of the electrical test setup. Three subpanels (100 A Load Center in Figure 3.5) were each supplied by one phase of a 75 kVA, 120/208 V wye transformer. A fused disconnect, with 100 A time-delay fuses, was installed between the subpanels and the transformer. These fuses were selected to minimize the chance of “blowing” on a short-term heavy overload as from a short-circuit in a sample cable or cord.

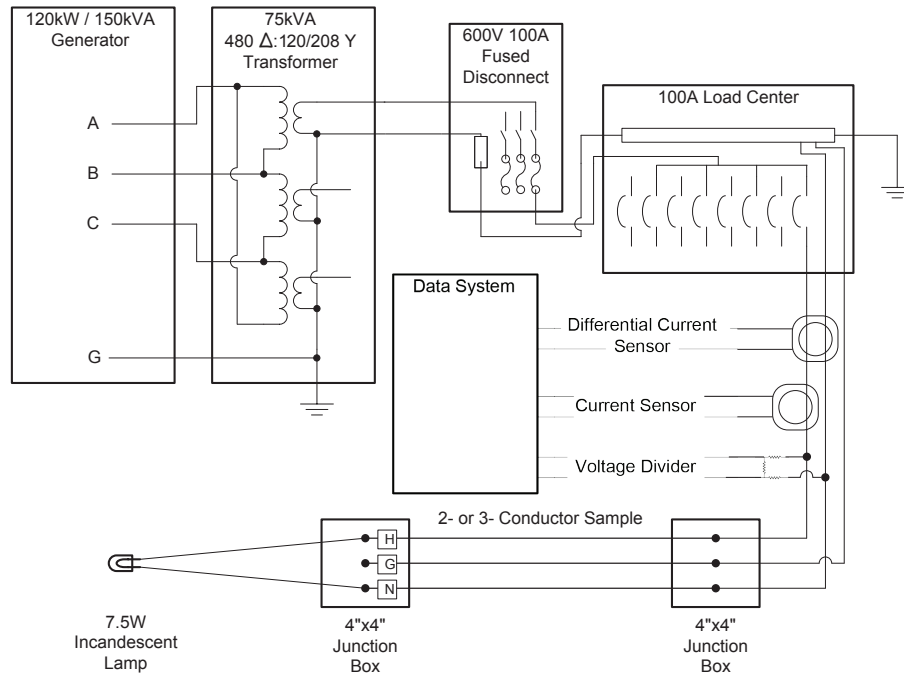


Figure 3.5: Line drawing schematic of the electrical test setup. The system was powered by 120 kW/150 kVA, 3-phase AC generator. Three subpanels (100 A load center) were each supplied by one phase of a 75 kVA, 120/208 V wye transformer with 100 A time-delay fuses installed between the subpanels and the transformer. 18 circuits were installed to examine 6 cords/cables and 3 circuit breakers which were equipped with a voltage sensing circuit that had a resistive voltage-divider to reduce signal levels for measurement purposes. Each circuit terminated at 7.5 W incandescent bulb for visual indication of live circuits. For 3-conductor circuits, the third insulated conductor was connected to the ‘hot.’

The available fault current in each circuit, calculated by loading the circuits and measuring voltage drop, ranged from 738 A to 752 A. Appendix A provides the data (Table A.1) and definitions (Table A.2) used to calculate the fault current within each of the circuits. Within each subpanel were two groups of three circuit breakers. Each group of three circuit breakers supplied specimens of one of the six cord types. For each cord/cable type, three different breakers were installed: a conventional thermal/magnetic breaker (MCCB), a ground-fault circuit interrupter (GFCI) breaker, and an arc-fault circuit interrupter (AFCI) breaker which also had a ground-fault protection built in. All of the circuit breakers were rated for 20 A. All of the 18 circuits were supplied through 5.49 m (18 ft) lengths of 14-2 NM-B cable with grounding conductors¹. The wiring samples were

¹These experiments were not specifically designed to directly assess the performance of circuit protection devices.

connected to the NM-B cable in individual electrical boxes installed beneath the floor and run up through openings in the floor. Each cord specimen had a length of 0.46 m (18 in) exposed above the floor. The cord/cable specimens were then run down through openings in the floor to another set of individual electrical boxes. From the second set of electrical boxes beneath the floor, 5.79 m (19 ft) lengths of 14-2 NM-B cable were run to 18 lamp sockets, each equipped with a 7.5 W incandescent bulb for visual indication of live circuits.

Note that in Figure 3.5 only one of the three circuit subpanels is shown. While only one sample is shown as ‘wired’ to a light bulb, all 18 samples were connected to an incandescent light bulb. Three subpanels, each supplied six samples which resulted in 18 total exposed cords per experiment.

Each of the 18 circuits were equipped with a voltage sensing circuit that had a resistive voltage-divider to reduce signal levels for measurement purposes. Gain levels were determined for all circuits with a resistive load between line and ground. Voltage measurements were utilized solely in determining the status of the circuit breakers, indicating either a closed or open condition. Clamp-on current sensors were used for measuring fault currents in the line (hot) wire, with gain levels determined by manufacturer’s specifications. Fault current measurements were utilized only in determining the cause of the circuit breaker trips. Finally, differential current sensors comparing the current in the line conductor to the current in the neutral conductor were used. A schematic of the measurements is included in Figure 3.5.

Gain levels were determined for all circuits with a resistive load between line and ground (Table B.1). As a result of the gain level measurements, differential current magnitude trip levels for all GFCI breakers were confirmed to be greater than 4 mA_{RMS} and less than 10 mA_{RMS}, while trip levels for all AFCI breakers were confirmed to be greater than 10 mA_{RMS}.

In circuits with 3-conductor cord specimens, a measured differential current would indicate ground-fault conditions, as the line and neutral currents would become unequal. The inequality in currents would indicate an alternate electrical path, specifically ground. In circuits with 2-conductor cord samples, no differential current could be measured, as there were no electrical paths to ground through the cable, however other pathways were possible. The system is center-tapped ground so there could be line-to-line faults or line-to another circuit’s neutral. Based on the spacing between samples and ‘tight’ install in the floor, line-to another circuit’s neutral was not expected. The data were collected with a computer-based data acquisition system that collected a thousand readings per second. The fast data collection rate was necessary to capture the shape of the electric waveforms so that the cause of the circuit fault could be determined.

Table 3.4 shows the breakdown of 18 configurations: circuit number, breaker type, and cord/cable type.

The results of this experiments may be different with different electrical configurations such as the 500 A available fault current and 15 m to 21 m (50-70 ft) home run length as defined by UL 1699.

Table 3.4: Electrical Fault Test Setup – Circuit, Breaker, and Cord/Cable

Circuit Number	Breaker Type	Cord/Cable Type
1	MCCB	18-2 SPT1
2	AFCI	18-2 SPT1
3	GFCI	18-2 SPT1
4	MCCB	16-3 SJTW
5	AFCI	16-3 SJTW
6	GFCI	16-3 SJTW
7	MCCB	12-2 NM-B
8	AFCI	12-2 NM-B
9	GFCI	12-2 NM-B
10	MCCB	12-3 NM-B
11	AFCI	12-3 NM-B
12	GFCI	12-3 NM-B
13	MCCB	18-3 SVT
14	AFCI	18-3 SVT
15	GFCI	18-3 SVT
16	MCCB	18-2 NISPT-2
17	AFCI	18-2 NISPT-2
18	GFCI	18-2 NISPT-2

In the cord/cable type column the first two numbers define the gauge (diameter) and the number of conductors in the cord/cable, respectively. The text string portion of the cord/cable type in Table 3.4 defines the insulation and temperature rating of the cords. The four cords and two cables tested had temperate ratings that ranged between 90 °C to 105 °C. Table 3.5 describes the insulation, voltage rating, and temperature rating of the cords and cable.

Table 3.5: Description of Cord/Cable Type Examined

Type	Insulation	Voltage Rating	Temperature Rating
SPT1 (cord)	Thermoplastic cord, parallel jacketed	300 V	105 °C
SJTW (cord)	Thermoplastic hard jacket, water resistant	300 V	105 °C
NM-B (cable)	Non-metallic sheathed, thermoplastic insulated	600 V	90 °C
SVT (cord)	Thermoplastic jacket, service vacuum	300 V	105 °C
NISPT-2 (cord)	Non-integral service parallel thermoplastic	300 V	105 °C

The cords and cables were installed on the floor of the structure, 0.45 m (18 in.) from the opening. The cords/cables were spaced 0.1 m (4 in.) apart on center with the first cord/cable 0.96 m (38 in.) from the left side wall. Each cord/cable had an exposure length of 0.45 m (18 in.). Figure 3.6 shows a photograph of the installed cords and cables prior to an experiment. Note the presence of heat flux gauges installed in the floor between every other cord/cable.

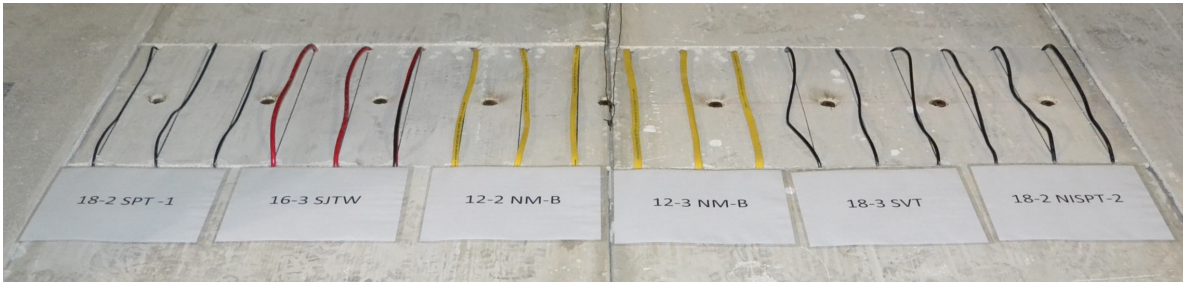


Figure 3.6: Photograph of the 18 cord/cable exposures in the test room prior to the start of the test. The placards identify the cord/cable type.

3.5 Test Procedure

All ignitions were started in the center seat cushion of the rear sofa with an electric match. The fires were allowed to grow until all of the circuits had faulted, at which point the power was disconnected and the fire suppressed with water. The suppression was conducted with a low flow nozzle, less than 20 gpm. The firefighters were directed to apply the water in a manner that would not impact the cord samples. After the fire was extinguished, the cords were photographed in place and then collected for further examination in the laboratory.

4 Results

4.1 Thermal Exposure

Figure 4.1 shows the heat release versus time for the six experiments. For the six experiments conducted, Experiments 1–3 were replicates (Table 3.1) of the two sofa fuel load. Experiments 4 and 5 were replicates using the reduced fuel load (single sofa) while Experiment 6 had an increased fuel load with the addition of MDF paneling to examine if the additional fuel load had different results.

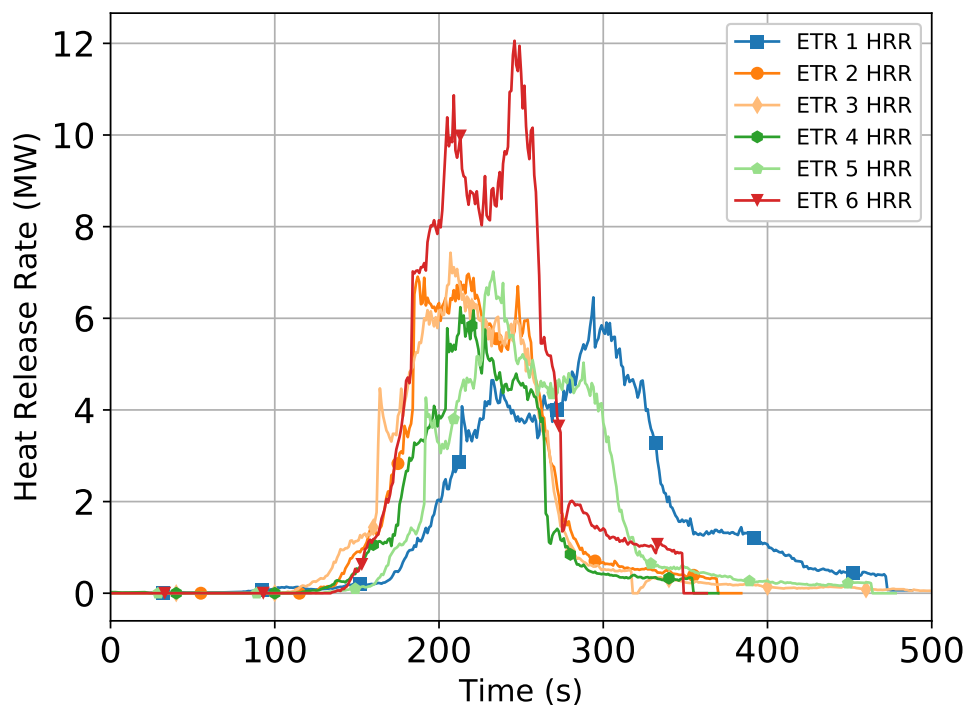


Figure 4.1: Heat release rate versus time replicates for each of the six experiments.

The heat release rate growth was similar for all six experiments as shown in Figure 4.1. The peak HRR values for Experiments 1–5, shown in Table 4.1, have a standard deviation of 475 kW, within the 11 % uncertainty measurement capability of the calorimeter of the laboratory. Recall the peak HRR of the sofa from Table 3.3 compared to peaks from the compartment experiments. In these experiments, the padding and capret as well as compartment effects contributed to the higher heat release rates. The removal of a sofa in Experiments 4 and 5 did not have a significant impact on peak release rate prior to suppression compared to Experiments 1–3 where two sofas were used. To further assess heat release, the data were integrated over time from ignition to time of first trip to calculate a total energy release for each experiment. Due to suppression actions, it was impractical to integrate over the total burn duration. The average total energy released prior to first trip was

245 MJ with a standard deviation of 28 MJ. The standard deviation is on par with the uncertainty measurement capability of the calorimeter of the laboratory. Table 4.1 also included the time of the first and last trip for each experiment which shows that the time between the trips ranged between 30 and 40 seconds.

Table 4.1: Peak HRR, Total Energy, and Time to Trip from the Room Experiments

Exp #	Peak HRR (MW) Prior to Suppression	Total Energy Released Prior to First Trip (MJ)	Time to First Trip (s)	Time to Last Trip (s)
1	6.5	285	267	314
2	7.0	264	205	235
3	7.4	220	202	236
4	6.2	211	210	235
5	7.0	245	238	267
6	12.0	244	206	245

For Experiment 6, however, the distribution of fuel within the compartment (fuel around the perimeter of the room and floor to ceiling) changed due the addition of MDF paneling on the walls. This led to an increase in burning exterior to the compartment as shown in the comparison images between Experiments 5 and 6 in Figure 4.2. Figure 4.2 shows the fire external to the room in both Experiments 5 and 6 prior to any of the circuits being tripped. Outside of Experiment 1, which had a slower initial growth as the fire initially burned in depth in the seat cushion versus burning into the back cushion; fire was first visible outside of the compartment at approximately 2:45 (165 s) after ignition. As all of the fuel loads were sufficient to transition the room to flashover, external burning was a product of excess fuel and the fixed ventilation opening.



Figure 4.2: Photographs of the room during flashover, prior to any of the circuits tripping - Experiment 5 (left) and Experiment 6 (right).

To limit unnecessary damage to the exposed cords after all circuits had tripped, the fires were suppressed rather than allow for all of the fuel to be consumed. This is noticeable in the sharp declines in HRR in Figure 4.1. For suppression, the stream was directed off of the ceiling and walls until the surfaces were cooled followed by directing the stream onto the burning contents for final extinguishment. Care was taken during suppression actions to avoid direct contact from the

stream to the exposed cord samples. Note, prior to suppression, power was disconnected from the circuits at the load center after the last circuit had tripped.

While there was consistency in the HRR growth for all experiments and peak values for Experiments 1–5, that measurement alone cannot quantify similarities in fire behavior within the room. This is due in part to the significant amount of combustion that occurred external to the room (Figure 4.2). Therefore, the mid-room thermocouple array was also used to assess the repeatability of the thermal conditions within the compartment. All six experiments showed similar temperature behavior, and Figure 4.3 shows the thermocouple time-history from Experiments 2 and 3 as representative examples.

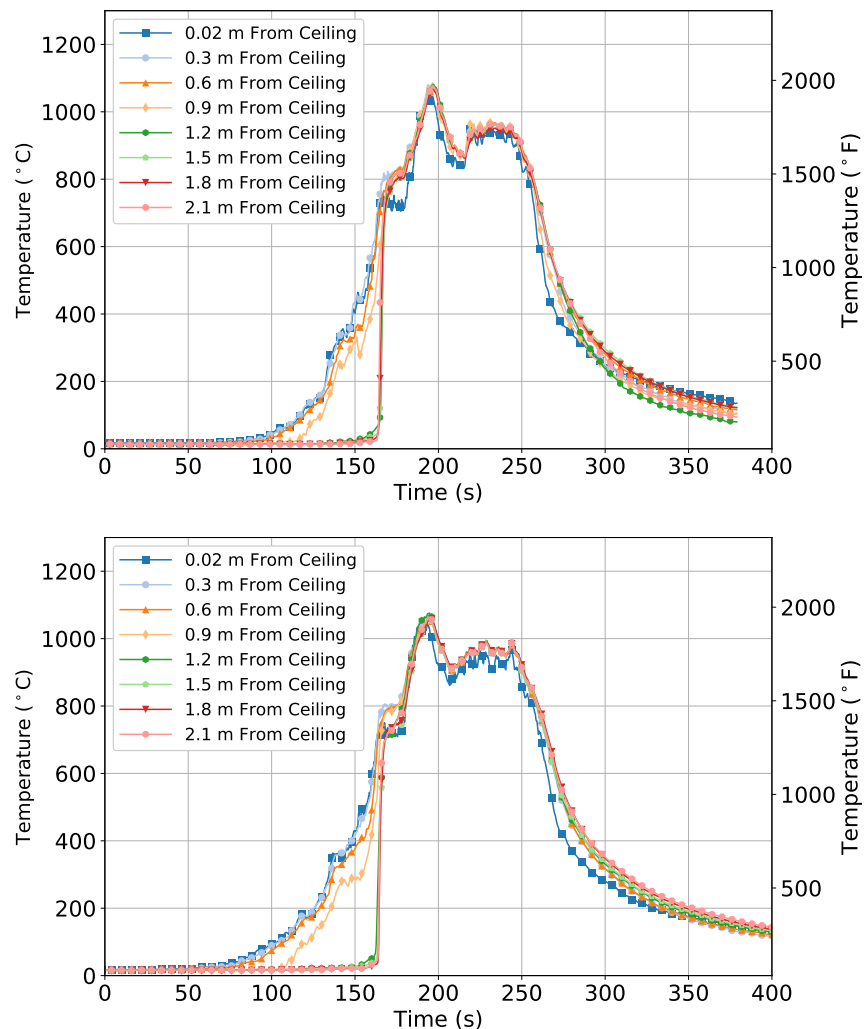


Figure 4.3: Experiment 2 (top) and Experiment 3 (bottom) – Thermocouple temperature time-history at the mid-room location.

To ensure that cords at the end positions (e.g. 1 and 18) did not “see” different heat fluxes compared to the cords in the center, it was important for the heat flux exposure at the floor to be spatially consistent. Consider the time history of heat flux for each gauge from Experiments 5 and 6, which

have the minimum and maximum fuel load, respectively. Figure 4.4 shows that while the peak values vary between the experiments (recall heat release data in Figure 4.1) the mean heat flux sits within the uncertainty of measurements.

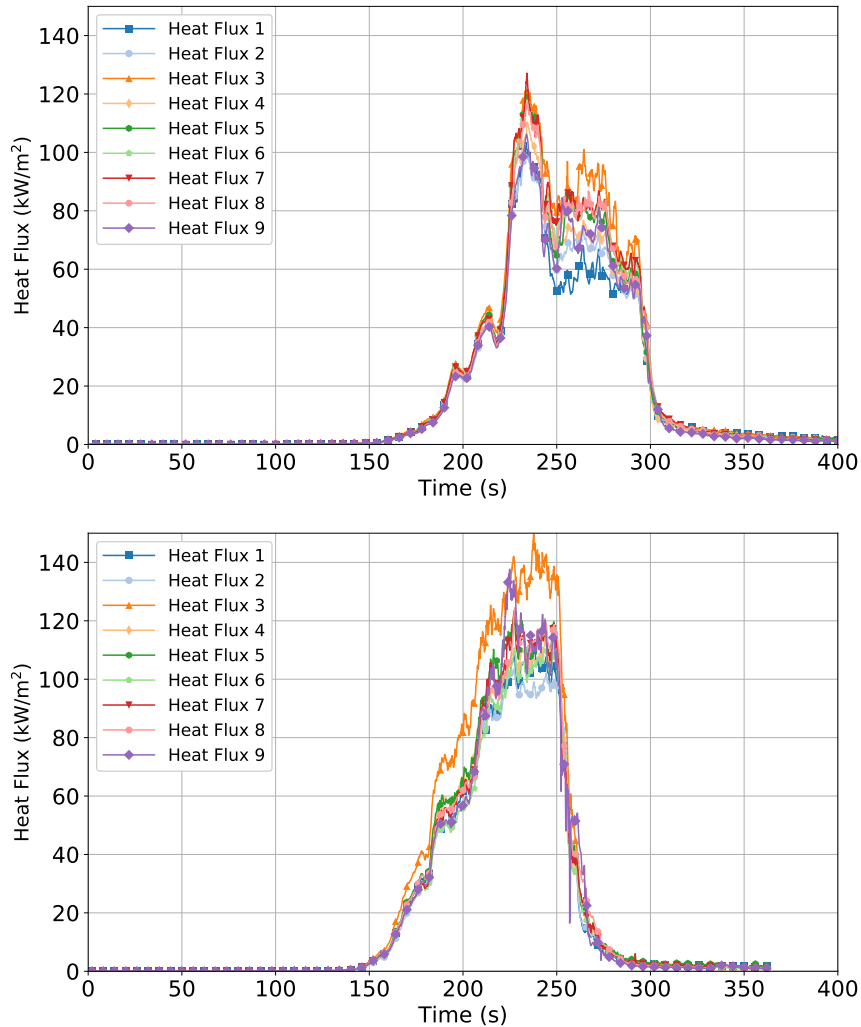


Figure 4.4: Experiment 5 (top) and Experiment 6 (bottom) – Heat flux time-history at the floor near the vent opening.

In Experiments 1, 2, and 3, however, there was debris that fell from the ceiling. The debris (Figure 4.5) landed overtop some of the heat flux gauges effectively lowering the heat flux measurement from the gauge. In Experiment 1, heat flux gauges 3 and 4 both had debris land on top of them. Figure 4.6 shows the lower values of gauges 3 and 4 through the time history of the experiment.



Figure 4.5: Experiment 1 – Debris falling from ceiling onto heat flux gauge 3.

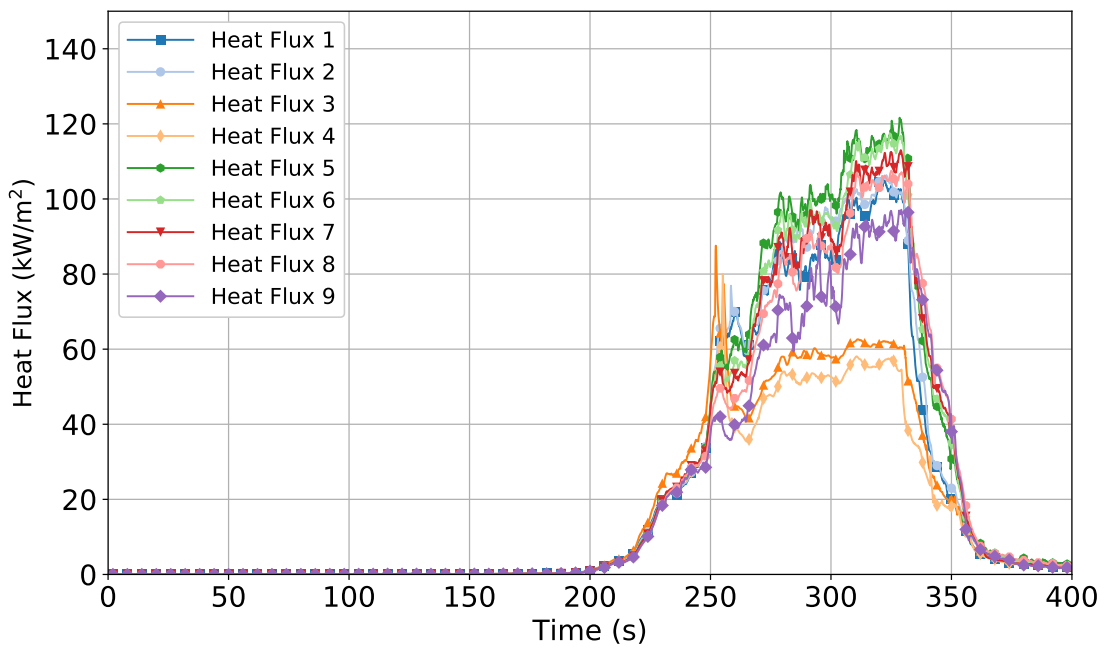


Figure 4.6: Experiment 1 – Heat flux time-history at the floor near the vent opening.

Since the remainder of the heat flux gauges were not covered by debris and Experiments 4, 5, and 6 showed that without debris the heat flux gauge is spatially consistent, cords 5 & 6 and 7 & 8 were mapped to the heat flux gauges 2 and 5, respectively. For Experiment 3, the heat flux gauges which were covered by debris were gauges 3 and 5. Cords 5 & 6 and 9 & 10 were mapped to heat flux

gauges 4 and 6, respectively. In Experiment 2, the debris was sufficient to impact a majority of the heat flux gauges. As a result, the heat flux data from Experiment 2 is not included in aggregate analysis. This did not preclude the electrical trip data from being analyzed. It is important to note that while debris fell during experiments, there was 0.46 m (18 in) of exposed cable for each cord and the majority of the cord remained exposed through the duration of the experiment.

4.2 Electrical Response

All of the breakers tripped on either high-current fault (over-current trip) or ground-fault conditions. An over-current trip occurred when the breaker cleared a fault within 1/2 electrical cycle due to a spike in current. An over-current trip was identified in the signal data by a spike in the current coupled with a drop in the voltage signal. A ground-fault trip was identified in the signal response with a current return to ground coupled with a drop in the voltage signal. While there was evidence of electrical arcing from the physical inspection of the wires (see Section ??), examination of the waveforms at the time as which the circuits tripped did not show signs of an arc fault such as the shouldering of the voltage signal. Figure 4.7 shows an over-current trip from Experiment 1 for Circuit 1: the 18-2 SPT1 cord with an MCCB.

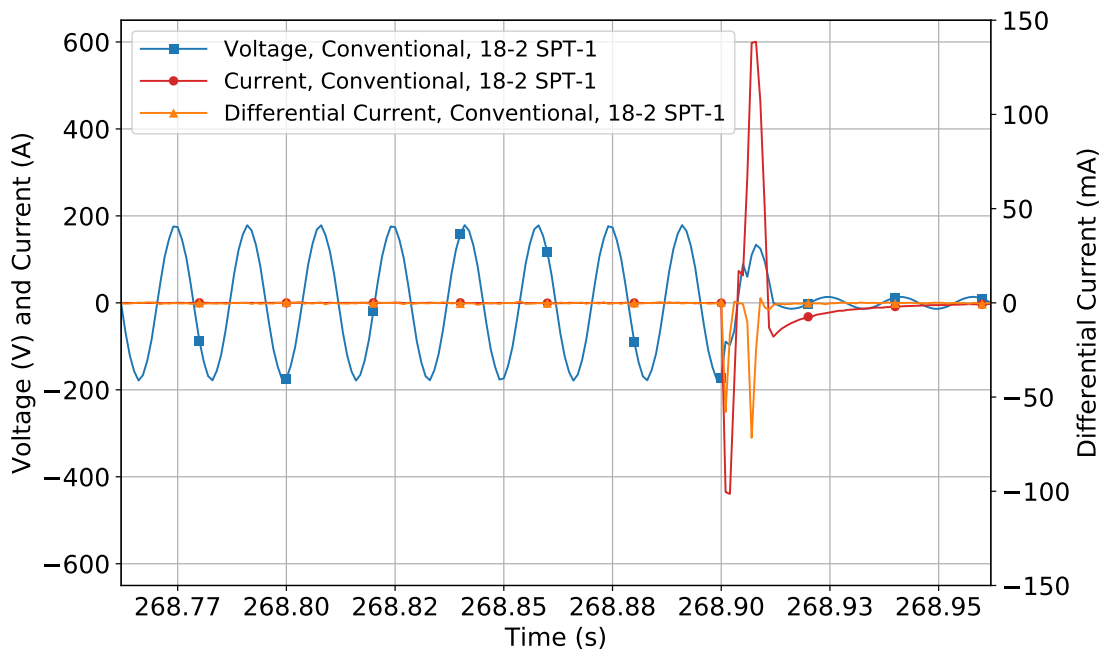


Figure 4.7: Experiment 1 – Signal data of an MCCB with 18-2 SPT1 cord (Circuit 1) that had an over-current trip.

No arc-fault trips were confirmed. Based on the electrical setup in these experiments (high supply current and AFCI at the panel board with a short homerun), these results were not unexpected. All of the AFCI breakers tripped either due to a ground-fault condition or due to a high-current fault. The brand and model of AFCI selected for these experiments, while not marketed as an

AFCI/GFCI, did have ground-fault detection incorporated within its arc fault detection algorithm. This helps the AFCI detect parallel arcing conditions for faults that arc from ungrounded to grounding conductor (three conductor cord, typically). It is important to recognize that this does not apply to all parallel arcs since they can also arc from line to neutral. However, the ground fault level for an AFCI may be set higher than the 5 mA +/- 1 mA level typical of residential GFCIs. The difference is because a GFCI is designed for personal protection while differential fault current detection in an AFCI is arc fault protection that happens to be a ground fault condition.

These experiments demonstrate the existence of ground-fault detection circuitry within the chosen AFCI breakers, as well as the difference in ground-fault trip levels between GFCI and AFCI breakers. Ground-fault trips were exclusively indicated with NM-B cable, and all NM-B cables with GFCI breakers tripped on ground faults. Figure 4.8 shows a ground-fault trip from Experiment 1 for the 12-2 NM-B cord with a GFCI breaker.

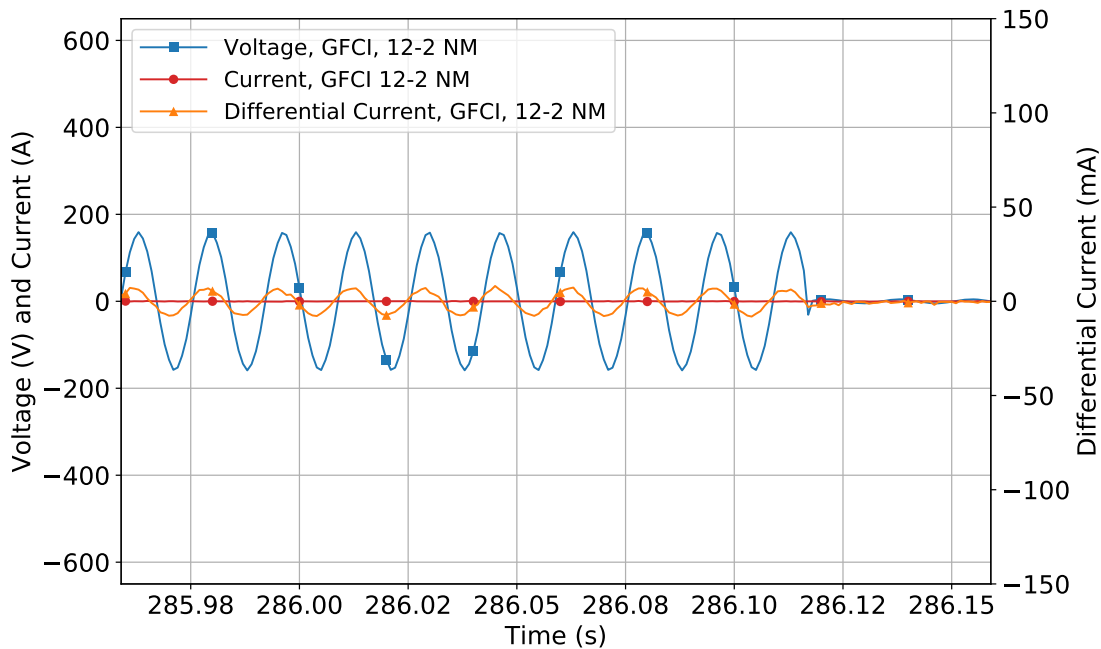


Figure 4.8: Experiment 1 – Signal data of a GFCI breaker with 12-2 NM-B cable (Circuit 9) that had a ground fault trip.

Note, not all NM-B circuits protected by AFCI breakers tripped on ground-faults. There were three examples of AFCI breakers with NM-B cable which tripped magnetically: Experiment 1 – 12-3 NM-B cable; Experiment 4 – 12-3 NM-B cable; and Experiment 5 – 12-2 NM-B cable. Data from these samples include high leakage currents, clipping of the differential current sensor signals, and current spikes of greater than 300 A ². Figure 4.9 shows that in Experiment 5, the 12-2 NM-B cable with an AFCI circuit, magnetically tripped with a current spike of 546 A. Also shown is the clipping of the differential current signal at 99.7 mA.

²Note that UL 489 does not control instantaneous trip levels. Had different circuits been chosen, the instantaneous trip levels may have been different.

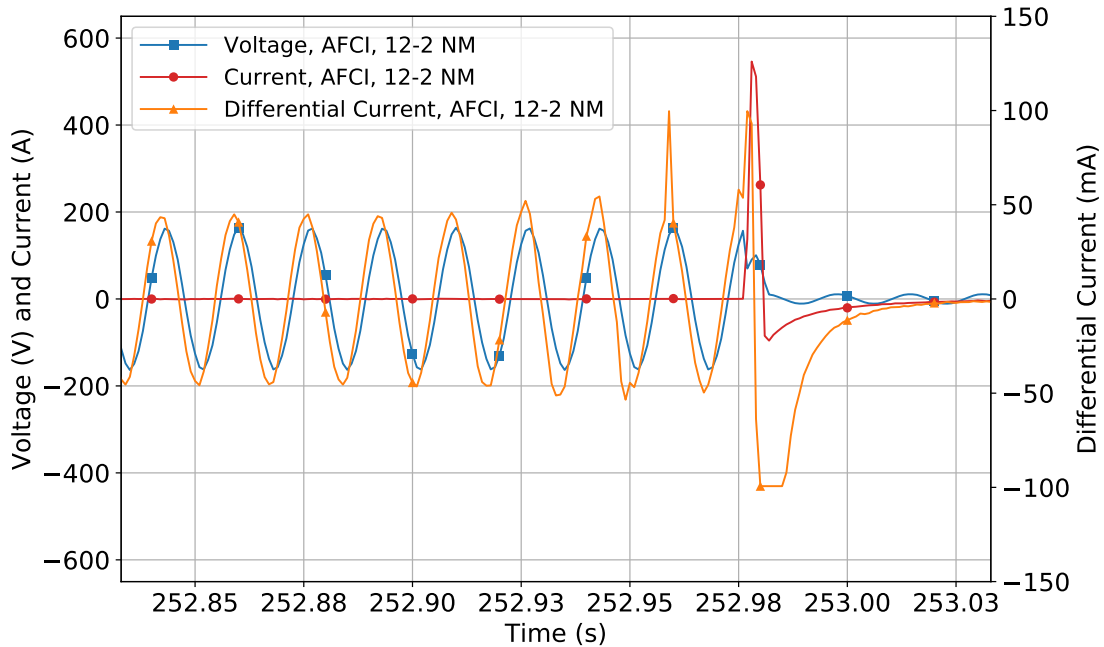


Figure 4.9: Experiment 5 – Signal data of a AFCI breaker with 12-2 NM-B cable (Circuit 8) that had an over-current trip.

Additionally, there were three cases (two AFCI, one MCCB) where 3-conductor cord could have potentially had a ground-fault failure had the circuit been a GFCI. Note, the ground-fault trip thresholds for the AFCI breakers were higher than for the GFCI breakers. Two of these cases occurred with SJTW cable (Experiment 1 – 16-3 SJTW, MCCB and Experiment 6 – 16-3 SJTW, AFCI) and one with an SVT cable (Experiment 2 – 18-3 SVT, AFCI). Figure 4.10 shows the voltage, current, and differential current for Experiment 6 – 16-3 SJTW with an AFCI breaker. In all three of these cases, there were escalating differential current prior to the magnetic trip as shown in Figure 4.10, as well as peak RMS differential current values over the ground-fault threshold for the GFCIs used. The experiments revealed that it cannot be assumed that because an AFCI or GFCI circuit tripped, that it was a result of an arc-fault or a ground-fault.

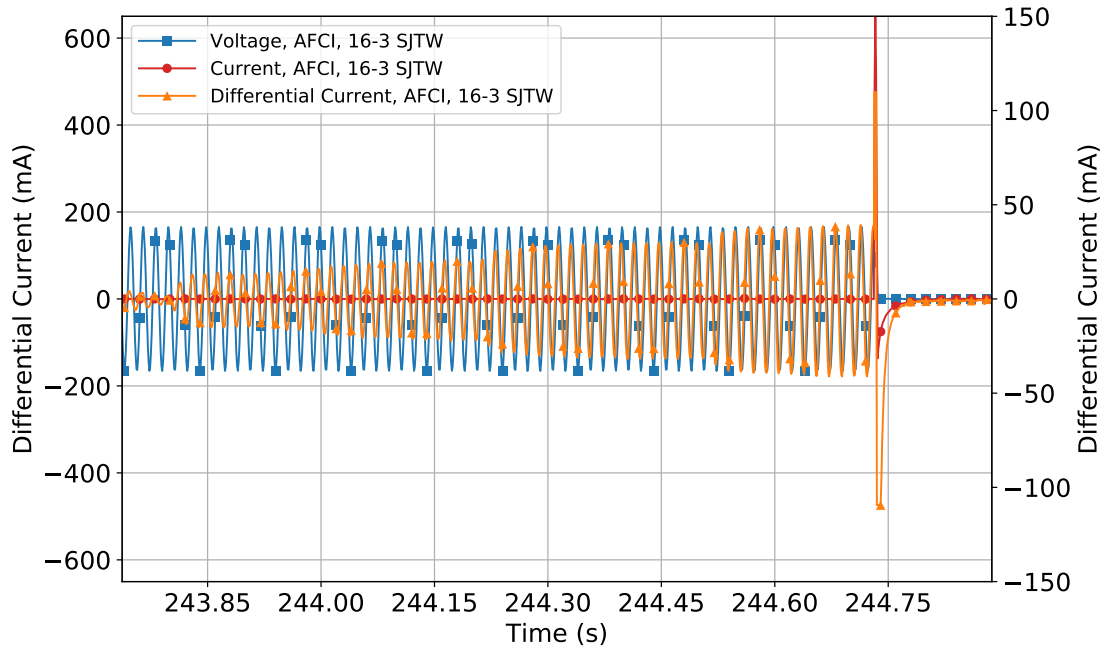


Figure 4.10: Experiment 6 – Signal data of a AFCI breaker with 16-3 SJTW cord (Circuit 5) that showed signs of a ground-fault but had an over-current trip.

In each of the six experiments, the 18-2 SPT-1 was the first cord to trip a circuit protection device and the 16-3 SJTW cord was the last. The circuit protection device types for the cords that tripped first and last varied by test. In other words, for the particular cords, one circuit device was not more or less susceptible to tripping. For an overall view of trip type for the 18 exposed cord/cable and breaker configurations, see Table 4.2. Additionally, specific trip data (time, heat flux, current, and differential current) for each configuration for each experiment is included in Appendix C in Tables C.1 – C.6. Note that time in Tables C.1 – C.6 is time from the ignition of the sofa which is not a the same as exposure time as there is a lag associated with fire growth of the sofa.

Table 4.2: Circuit Trip Type for Each Cord/Cable and Break for Each Experiment

Circuit Number	Breaker Type	Cord/Cable Type	Trip Type					
			Exp 1	Exp 2	Exp 3	Exp 4	Exp 5	Exp 6
1	MCCB	18-2 SPT1	OC	OC	OC	OC	OC	OC
2	AFCI	18-2 SPT1	OC	OC	OC	OC	OC	OC
3	GFCI	18-2 SPT1	OC	OC	OC	OC	OC	OC
4	MCCB	16-3 SJTW	OC	OC	OC	OC	OC	OC
5	AFCI	16-3 SJTW	OC	OC	OC	OC	OC	OC
6	GFCI	16-3 SJTW	OC	OC	OC	OC	OC	OC
7	MCCB	12-2 NM-B	OC	OC	OC	OC	OC	OC
8	AFCI	12-2 NM-B	GF	GF	GF	GF	OC	GF
9	GFCI	12-2 NM-B	GF	GF	GF	GF	GF	GF
10	MCCB	12-3 NM-B	OC	OC	OC	OC	OC	OC
11	AFCI	12-3 NM-B	OC	GF	GF	OC	GF	GF
12	GFCI	12-3 NM-B	GF	GF	GF	GF	GF	GF
13	MCCB	18-3 SVT	OC	OC	OC	OC	OC	OC
14	AFCI	18-3 SVT	OC	OC	OC	OC	OC	OC
15	GFCI	18-3 SVT	OC	OC	OC	OC	OC	OC
16	MCCB	18-2 NISPT-2	OC	OC	OC	OC	OC	OC
17	AFCI	18-2 NISPT-2	OC	OC	OC	OC	OC	OC
18	GFCI	18-2 NISPT-2	OC	OC	OC	OC	OC	OC

OC = Over-Current Trip, GF = Ground-Fault Trip

5 Discussion

5.1 Heat Flux Analysis

The time history of heat flux provided insight into exposure, specifically the rapid rise in heat flux as the compartment transitioned to flashover. One indicator for flashover is a heat flux of 20 kW/m^2 [15]. While the lowest instantaneous heat flux at the time of trip being greater than 70 kW/m^2 indicates that flashover likely occurred, the instantaneous heat flux does not completely describe the exposure. A time integrated heat flux which quantifies the duration exposure until the circuit breaker tripped is a more meaningful description. Recall from Figure 4.4, the temporal heat flux data from Experiments 5. The heat flux grew until peak heat fluxes occurred at approximately 225 s post ignition and then dropped to fairly steady values for 50 s before suppression actions were taken after 300 s. In Experiment 5, the earliest trip occurred at 237 s post ignition (see Table C.5), approximately 12 s after the peak values were reached. Table 5.1 shows the average integrated heat flux and standard deviation as function of the six exposed cord types.

Table 5.1: Mean and Standard Deviation of Integrated Heat Flux for Each Cord Type at Trip

Cord Type	Integrated Heat Flux	
	Mean (MJ/m^2)	Std. Dev (MJ/m^2)
18-2 SPT1	22.8	4.6
16-3 SJTW	48.9	9.4
12-2 NM-B	35.3	4.8
12-3 NM-B	35.9	8.9
18-3 SVT	28.4	3.7
18-2 NISPT-2	30.7	4.4

It was not expected that different cords, with different thermal masses, would behave the same way when exposed to heat. The measured integrated heat flux data in Table 5.1 shows overlap in the data for the post-flashover exposures. One note is that circuits connected in series to the 18-2 SPT1 cord tripped first and the circuits connected in series to the 16-3 SJTW cord were the last to trip. The integrated heat fluxes ranges corresponding to these times, did not overlap.

Novak tested energized 14-2 NM-B cables, which were similar to the 12-2 NM-B cables used in this study in terms of both having $90 \text{ }^\circ\text{C}$ ($194 \text{ }^\circ\text{F}$) rated conductor insulation enclosed within an overall non-metallic flame retardant PVC jacket. Novak exposed the energized cables to steady state radiant heat fluxes that ranged from 22 to 55 kW/m^2 . Above 26 kW/m^2 , Novak's data showed a significant decrease in time to failure of the cables [7, 16]. Integrating the heat flux exposure from Novak's set of tests yielded a mean of 17.3 MJ/m^2 with a standard deviation of 9.2 MJ/m^2 . The total exposure energy needed to result in a fault was approximately one half of the values for the NM-B cables used in this current study.

Based on the information from the Safety Engineering Laboratories study on appliance power cords (SPT-1 and SPT-2) exposed to a steady state 40 kW/m^2 radiant exposure [6], the range of total heat exposures ranged from 9.6 MJ/m^2 to 15.8 MJ/m^2 . Although a one to one comparison can't be made, the appliance power cords tested in the current set of experiments had mean total heat exposure values ranging from 22.8 MJ/m^2 to 30.7 MJ/m^2 . It is of interest that the peak values from the compartment fire experiments were more than twice the values of the bench scale steady state exposures.

5.2 Physical Inspection of Cords

Further analysis on potential correlations between circuit trip type, cord type, and thermal exposure was conducted by physical examination of the cords under a microscope following each experiment. Figure 5.1 is a photograph of the exposed cords still in place following Experiment 2. The placards in front of the cords identify the cord type.



Figure 5.1: Photograph of the 18 cord exposures in the test room following Experiment 2. The placards identify the cord type.

Following each experiment, the remains of each cord were carefully removed from the floor to limit potential damage to the cords to only that which was caused by the fire. Each cord was cleaned to remove large debris. The cords were then photographed using an 8x magnification digital microscope. From these images, beads, notches, and broken strands were able to be clearly identified. The damage to the conductors was consistent with electrical arcing. Figure 5.2 shows an example of a bead and notch that formed in a 12-2 NM-B conductor that had a magnetic trip in Experiment 2.



Figure 5.2: Magnified photograph of the 12-2 NM-B cable on a thermal magnetic circuit breaker following Experiment 2 showing both a bead and a notch on the cable.

Examination of the cord photographs did not yield any trend with respect to whether beads/notches/broken strands were present in cords that tripped magnetically or with a ground fault. Additionally, there were no trends with respect to cord type and visual damage. Consider the following post exposure magnified photographs (Figures 5.3-5.5). All of these images are of 16-3 SJTW cord; there are two images of each circuit type as well as one image from each experiment. Figures 5.3, 5.4, and 5.5 show pairs of magnified, post-experiment images of the 16-3 SJTW cord with thermal magnetic circuit breaker, AFCI, and GFCI protection respectively. While some broken strands and larger beads were visible without magnification, the use of a digital microscope provided a more complete assessment of the damage to the cords.



Figure 5.3: Magnified photograph of the 16-3 SJTW cord on a thermal magnetic circuit breaker following Experiment 1 (top) and Experiment 5 (bottom).

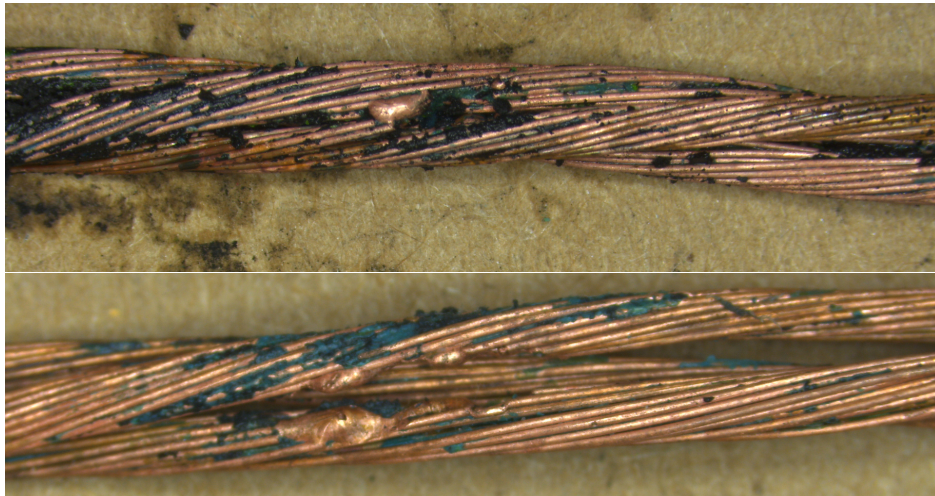


Figure 5.4: Magnified photograph of the 16-3 SJTW cord on an AFCI following Experiment 2 (top) and Experiment 6 (bottom).

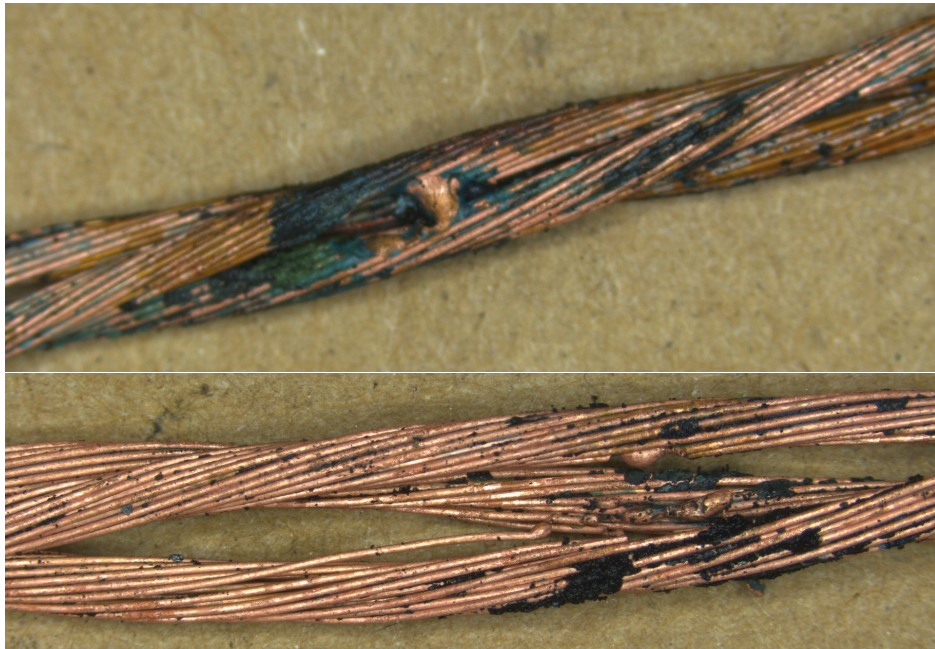


Figure 5.5: Magnified photograph of the 16-3 SJTW cord on a GFCI following Experiment 3 (top) and Experiment 4 (bottom).

Two of the images are from circuits that were considered outliers from the signal analysis (Experiment 1, MCCB and Experiment 6, AFCI). There are no visual cues from any post-experiment images in Figures 5.3–5.5 that would indicate different behavior. Beading and broken strands were not unique to any particular circuit protection. For an overview of the damage to each cord for all of the experiments, see Table D.1 in Appendix D.

6 Future Research Needs

These experiments exposed energized electrical cords/cables to compartment fire conditions. The placement of the cords and cables at the opening of the compartment provided the most severe exposure. As the compartment fire transitioned to flashover the heat flux exposure to the cords on the floor ignited the thermoplastic insulation of the cords. An extension of these experiments would be to change the exposure location. Does depth in the room, where the exposure would be less severe have an impact on the electrical response or physical performance of the cables and cords? The second variable is ventilation. Ventilation is known to impact fire patterns [17]. Cord and cable performance as a function of exposure location and ventilation could help inform fire investigators as well as the impact of combustible interior finishes.

These experiments only examined one electrical configuration and the circuit protection devices were remote from the exposure. The configuration was limited in that the high available current and short homerun distance would not be used if the configuration was designed to UL 1699. As a result, conducting experiments to examine consistency of circuit trips with similar thermal exposures but varied electrical configurations could provide valuable information to fire investigation community.

7 Summary

This set of experiments was conducted to examine the response of energized cords and different types of circuit protection devices to a growing compartment fire. Four cord types (18-2 SPT1, 16-3 SJTW, 18-3 SVT, 18-2 NISPT-2) and two cable types (12-2 NM-B, 12-3 NM-B) as well as three types of circuit protection (MCCB, AFCI, GFCI) were subjected to six room-scale fire exposures. The six room fires consisted of three replicate fires with two sofas as the main fuel components, two replicate fires with one sofa as the main fuel component and one fire with two sofa and vinyl-covered MDF paneling on three walls of the room. Compared to prior work, each of the fuel packages was sufficient to support flashover conditions in the room and as a result, the exposures in these experiments could be characterized as faster and more severe.

All of the circuits faulted in each of the experiments by either an over-current trip or a ground-fault trip. While all three circuit types tripped in every experiment, it cannot be assumed that an arc-fault or ground-fault caused an AFCI or GFCI circuit to trip. The only cord types that tripped with a ground-fault were the non-metallic sheathed (12-2 NM-B and 12-3 NM-B) cables. This was likely due to the presence of a bare grounding conductor. Assessments of both thermal exposure and physical damage did not reveal any correlation between the total integrated heat flux exposure or the type/magnitude of damage (broken strands, beads, notches) and the signal response (trip type).

For the fire investigator, with regard to the thermal exposure prior to the circuit trip, in each case, the heat flux exposure was in excess of 70 kW/m^2 and the insulation was burning prior to the trip. Further no correlation could be found between the post-fire damage on the exposed samples and the type of circuit protection device it was connected to.

References

- [1] National Fire Protection Association, Quincy, Massachusetts. *NFPA 921, Guide for Fire and Explosion Investigations*, 2017.
- [2] NIJ Forensic Science Technology Working Group. Technology Working Group Operational Requirements. <https://www.nij.gov/topics/forensics/documents/2014-forensic-twg-table.pdf>, 2014.
- [3] B. Béland. Examination of Electrical Conductors Following a Fire. *Fire Technology*, 16(4):252–258, 1980.
- [4] B. Béland. Arcing Phenomenon as Related to Fire Investigation. *Fire Technology*, 17(3):189–201, 1981.
- [5] B. Béland. Considerations on Arcing as a Fire Cause. *Fire Technology*, 18(2):188–202, 1982.
- [6] J.M. Hoffman, D. J. Hoffmann, E.C. Kroll, J.W. Wallace, and M.J. Kroll. Electrical Power Cord Damage from Radiant Heat and Fire Exposure. *Fire Technology*, 34(1):29–42, 2001.
- [7] C. Novak, S. Stoliarov, M. Keller, and J. Quintiere. An Analysis of Heat Flux Induced Arc Formation in a Residential Electrical Cable. *Fire Safety Journal*, 55:61–68, 2013.
- [8] V. Babrauskas. Arc Mapping: A Critical Review. *Fire Technology*, 54:749–780, 2018.
- [9] National Fire Protection Association, Quincy, Massachusetts. *NFPA 70, National Electrical Code*, 2017.
- [10] W.M. Pitts, A.V. Murthy, J.L. de Ris, J. Filtz, K. Nygård, D. Smith, and I. Wetterlund. Round robin study of total heat flux gauge calibration at fire laboratories. *Fire Safety Journal*, 41(6):459–475, 2006.
- [11] L.G. Blevins. Behavior of bare and aspirated thermocouples in compartment fires. In *National Heat Transfer Conference, 33rd Proceedings*, pages 15–17, 1999.
- [12] W.M. Pitts, E. Braun, R. Peacock, H. Mitler, E. Johnson, P. Reneke, and L.G. Blevins. Temperature uncertainties for bare-bead and aspirated thermocouple measurements in fire environments. *ASTM Special Technical Publication*, 1427:3–15, 2003.
- [13] C. Huggett. Estimation of Rate of Heat Release by Means of Oxygen Consumption Measurements. *Fire and Materials*, 4(2):61–65, 1980.
- [14] R.A. Bryant and G. Mullholland. A Guide to Characterizing Heat Release Rate Measurement Uncertainty for Full-Scale Fire Tests. *Fire and Materials*, 32:121–139, 2008.
- [15] R. D. Peacock, P. Reneke, R. W. Bukowski, and V. Babrauskas. Defining flashover for fire hazard calculations. *Fire Safety Journal*, 32(4):331–345, 1999.

- [16] C. Novak. An Analysis of Heat-Flux Induced Arc Formation in a Residential Electrical Cables. Master's Thesis, University of Maryland, College Park, Maryland, 2001.
- [17] D. Madrzykowski and C. Weinschenk. Impact of fixed ventilation on fire damage patterns in full-scale structures, April 2019.

Appendix A Available Fault Current

Table A.1: Available Fault Current Data

Circuit	V_{open} (V)	V_{low} (V)	A_{low} (A)	V_{high} (V)	A_{high} (A)	Circuit Impedance (Ω)	Available Fault Current (A)
Phase A	120.57	120.36	1.1102	118.81	600.4	0.1634	738
Phase B	120.76	120.57	1.1076	119.04	-453.9	0.1606	752
Phase C	120.74	120.50	1.1099	118.95	599.7	0.1628	741

Table A.2: Fault Current Calculation Definitions

Variable	Definition
V_{open}	Voltage - Open Circuit
V_{low}	Voltage - Closed Circuit, Low Current Load
A_{low}	Amperage - Low Current Load
V_{high}	Voltage - Closed Circuit, High Current Load
A_{high}	Amperage - High Current Load
Circuit Impedance (Ω)	$(V_{\text{low}} - V_{\text{high}}) / (A_{\text{high}} - A_{\text{low}})$
Available Fault Current	V_{open} / Ω

Appendix B Gain Calculations

Table B.1: Gain Calculations

Circuit #	Decade Setting (Ω)	Metered mA _{RMS}	Metered mV _{RMS}	Calculated Gain
1	12010	10.0	10.73	0.932
2	12010	10.0	10.66	0.938
3	30040	4.0	4.48	0.894
4	12010	10.0	11.06	0.904
5	12010	10.0	9.62	1.040
6	30040	4.0	4.66	0.859
7	12010	10.0	9.41	1.063
8	12010	10.0	10.59	0.944
9	30040	4.0	4.11	0.974
10	12010	10.0	10.35	0.966
11	12010	10.0	10.88	0.919
12	30040	4.0	4.37	0.916
13	12010	10.0	10.70	0.935
14	12010	10.0	10.95	0.913
15	30040	4.0	4.42	0.905
16	12010	10.0	10.92	0.916
17	12010	10.0	11.06	0.904
18	30040	4.0	4.50	0.890

Appendix C Fault Data

Table C.1: Circuit Trip Data for Experiment 1

Circuit #	Breaker Type	Cord/Cable Type	Time (s)	Integrated		Diff. Curr. (mA)	Trip Type
				Heat Flux (MJ/m ²)	Current (A)		
1	MCCB	18-2 SPT1	268.9	19.2	600.4	-71.7	Over-Current
2	AFCI	18-2 SPT1	267.2	18.0	-453.9	-6.8	Over-Current
3	GFCI	18-2 SPT1	268.1	18.9	599.7	3.3	Over-Current
4	MCCB	16-3 SJTW	313.8	60.0	687.6	95.5	Over-Current
5	AFCI	16-3 SJTW	299.5	47.8	643.8	109.8	Over-Current
6	GFCI	16-3 SJTW	304.3	52.6	591.4	90.7	Over-Current
7	MCCB	12-2 NM-B	298.0	30.6	585.6	112.2	Over-Current
8	AFCI	12-2 NM-B	300.2	31.7	31.7	79.4	Ground Fault
9	GFCI	12-2 NM-B	286.1	34.5	-6.6	8.1	Ground Fault
10	MCCB	12-3 NM-B	304.0	52.3	-585.2	102.0	Over-Current
11	AFCI	12-3 NM-B	305.0	50.6	687.6	-68.7	Over-Current
12	GFCI	12-3 NM-B	283.5	30.4	-3.1	8.2	Ground Fault
13	MCCB	18-3 SVT	283.3	29.3	447.4	-98.4	Over-Current
14	AFCI	18-3 SVT	288.1	33.2	460.3	96.4	Over-Current
15	GFCI	18-3 SVT	283.0	26.7	573.3	-11.2	Over-Current
16	MCCB	18-2 NISPT-2	289.1	31.7	503.5	-4.6	Over-Current
17	AFCI	18-2 NISPT-2	283.4	24.1	-515.4	11.0	Over-Current
18	GFCI	18-2 NISPT-2	288.4	27.4	503.5	-7.4	Over-Current

Table C.2: Circuit Trip Data for Experiment 2

Circuit #	Breaker Type	Cord/Cable Type	Time (s)	Integrated		Diff. Curr. (mA)	Trip Type
				Heat Flux (MJ/m ²)	Current (A)		
1	MCCB	18-2 SPT1	209.9	23.9	623.2	-98.1	Over-Current
2	AFCI	18-2 SPT1	204.6	19.8	540.8	-19.3	Over-Current
3	GFCI	18-2 SPT1	205.5	16.6	-392.0	10.0	Over-Current
4	MCCB	16-3 SJTW	233.8	33.0	-533.1	95.5	Over-Current
5	AFCI	16-3 SJTW	235.9	44.5	578.5	109.8	Over-Current
6	GFCI	16-3 SJTW	227.9	37.3	549.5	-90.4	Over-Current
7	MCCB	12-2 NM-B	230.3	30.4	-625.2	112.2	Over-Current
8	AFCI	12-2 NM-B	223.5	26.6	-2.4	-73.0	Ground Fault
9	GFCI	12-2 NM-B	217.1	33.5	-1.4	8.0	Ground Fault
10	MCCB	12-3 NM-B	226.5	42.2	-580.7	102.0	Over-Current
11	AFCI	12-3 NM-B	225.8	24.5	-2.4	-72.6	Ground Fault
12	GFCI	12-3 NM-B	211.6	17.6	1.8	-8.1	Ground Fault
13	MCCB	18-3 SVT	217.7	19.8	-541.1	98.7	Over-Current
14	AFCI	18-3 SVT	219.8	20.8	-588.1	96.4	Over-Current
15	GFCI	18-3 SVT	216.5	23.1	-547.6	-24.3	Over-Current
16	MCCB	18-2 NISPT-2	220.6	25.4	464.2	4.1	Over-Current
17	AFCI	18-2 NISPT-2	224.9	25.3	437.4	-2.0	Over-Current
18	GFCI	18-2 NISPT-2	221.8	23.8	-553.7	-13.2	Over-Current

Table C.3: Circuit Trip Data for Experiment 3

Circuit #	Breaker Type	Cord/Cable Type	Time (s)	Integrated		Diff. Curr. (mA)	Trip Type
				Heat Flux (MJ/m ²)	Current (A)		
1	MCCB	18-2 SPT1	207.3	21.2	549.5	98.4	Over-Current
2	AFCI	18-2 SPT1	202.0	17.2	541.1	-14.7	Over-Current
3	GFCI	18-2 SPT1	217.0	30.4	-472.5	5.1	Over-Current
4	MCCB	16-3 SJTW	235.6	45.9	-669.0	95.5	Over-Current
5	AFCI	16-3 SJTW	228.6	41.3	443.6	-109.5	Over-Current
6	GFCI	16-3 SJTW	233.7	45.6	579.4	90.7	Over-Current
7	MCCB	12-2 NM-B	227.2	40.1	-461.3	112.2	Over-Current
8	AFCI	12-2 NM-B	235.0	46.8	-2.1	-76.0	Ground Fault
9	GFCI	12-2 NM-B	212.1	28.4	-1.8	-7.9	Ground Fault
10	MCCB	12-3 NM-B	216.9	32.6	539.5	102.0	Over-Current
11	AFCI	12-3 NM-B	218.5	34.1	-3.7	-71.6	Ground Fault
12	GFCI	12-3 NM-B	215.0	31.0	-2.7	-7.9	Ground Fault
13	MCCB	18-3 SVT	214.5	29.5	-419.1	2.0	Over-Current
14	AFCI	18-3 SVT	218.3	33.0	-574.6	96.4	Over-Current
15	GFCI	18-3 SVT	218.1	28.8	570.8	-94.2	Over-Current
16	MCCB	18-2 NISPT-2	229.3	37.4	347.3	5.0	Over-Current
17	AFCI	18-2 NISPT-2	219.1	31.0	494.1	-3.2	Over-Current
18	GFCI	18-2 NISPT-2	224.6	36.1	-422.9	13.3	Over-Current

Table C.4: Circuit Trip Data for Experiment 4

Circuit #	Breaker Type	Cord/Cable Type	Time (s)	Integrated		Diff. Curr. (mA)	Trip Type
				Heat Flux (MJ/m ²)	Current (A)		
1	MCCB	18-2 SPT1	217.3	28.2	558.5	-98.1	Over-Current
2	AFCI	18-2 SPT1	209.5	21.7	503.8	-19.9	Over-Current
3	GFCI	18-2 SPT1	211.2	24.6	418.4	-13.5	Over-Current
4	MCCB	16-3 SJTW	233.8	42.9	-370.5	95.5	Over-Current
5	AFCI	16-3 SJTW	234.6	50.6	-695.0	109.8	Over-Current
6	GFCI	16-3 SJTW	235.1	51.1	545.3	90.7	Over-Current
7	MCCB	12-2 NM-B	227.5	38.6	603.9	112.2	Over-Current
8	AFCI	12-2 NM-B	225.8	37.1	-20.8	-76.2	Ground Fault
9	GFCI	12-2 NM-B	218.3	33.6	-6.0	-7.6	Ground Fault
10	MCCB	12-3 NM-B	223.7	38.6	-563.0	102.0	Over-Current
11	AFCI	12-3 NM-B	227.0	39.7	570.8	97.0	Over-Current
12	GFCI	12-3 NM-B	218.1	32.2	-6.9	-8.0	Ground Fault
13	MCCB	18-3 SVT	214.3	30.0	649.0	-5.7	Over-Current
14	AFCI	18-3 SVT	216.3	31.8	-457.4	96.4	Over-Current
15	GFCI	18-3 SVT	214.9	25.9	388.8	-95.2	Over-Current
16	MCCB	18-2 NISPT-2	218.1	28.3	-406.8	-13.6	Over-Current
17	AFCI	18-2 NISPT-2	218.5	33.9	572.0	-3.9	Over-Current
18	GFCI	18-2 NISPT-2	218.3	33.6	-480.6	19.2	Over-Current

Table C.5: Circuit Trip Data for Experiment 5

Circuit #	Breaker Type	Cord/Cable Type	Time (s)	Integrated		Diff. Curr. (mA)	Trip Type
				Heat Flux (MJ/m ²)	Current (A)		
1	MCCB	18-2 SPT1	237.4	24.7	-637.4	-98.1	Over-Current
2	AFCI	18-2 SPT1	242.0	29.0	-649.3	-98.7	Over-Current
3	GFCI	18-2 SPT1	237.9	24.5	-514.4	-6.7	Over-Current
4	MCCB	16-3 SJTW	261.5	41.4	578.5	95.5	Over-Current
5	AFCI	16-3 SJTW	255.6	45.2	-661.2	109.8	Over-Current
6	GFCI	16-3 SJTW	266.8	55.1	-531.1	90.7	Over-Current
7	MCCB	12-2 NM-B	254.6	39.1	-644.8	112.2	Over-Current
8	AFCI	12-2 NM-B	253.0	37.9	546.0	99.7	Over-Current
9	GFCI	12-2 NM-B	245.7	35.1	-8.5	-7.5	Ground Fault
10	MCCB	12-3 NM-B	260.2	46.0	659.9	102.0	Over-Current
11	AFCI	12-3 NM-B	248.1	36.5	1.8	-68.8	Ground Fault
12	GFCI	12-3 NM-B	240.9	30.3	-26.6	-7.8	Ground Fault
13	MCCB	18-3 SVT	239.5	29.6	518.3	-2.2	Over-Current
14	AFCI	18-3 SVT	240.7	30.8	563.3	-96.4	Over-Current
15	GFCI	18-3 SVT	241.0	29.4	-503.4	-23.5	Over-Current
16	MCCB	18-2 NISPT-2	244.5	32.5	443.6	4.4	Over-Current
17	AFCI	18-2 NISPT-2	243.6	29.3	-541.4	-9.1	Over-Current
18	GFCI	18-2 NISPT-2	243.1	29.1	444.5	-13.9	Over-Current

Table C.6: Circuit Trip Data for Experiment 6

Circuit #	Breaker Type	Cord/Cable Type	Time (s)	Integrated		Diff. Curr. (mA)	Trip Type
				Heat Flux (MJ/m ²)	Current (A)		
1	MCCB	18-2 SPT1	205.5	18.2	466.4	-98.1	Over-Current
2	AFCI	18-2 SPT1	210.5	21.9	-550.5	-8.8	Over-Current
3	GFCI	18-2 SPT1	223.0	32.1	521.5	-17.9	Over-Current
4	MCCB	16-3 SJTW	240.6	49.4	-540.5	-95.1	Over-Current
5	AFCI	16-3 SJTW	244.7	74.0	655.1	109.8	Over-Current
6	GFCI	16-3 SJTW	236.1	61.9	-566.2	90.7	Over-Current
7	MCCB	12-2 NM-B	228.2	40.8	543.4	112.2	Over-Current
8	AFCI	12-2 NM-B	223.0	35.3	-2.1	-86.9	Ground Fault
9	GFCI	12-2 NM-B	223.0	36.4	-2.7	-7.9	Ground Fault
10	MCCB	12-3 NM-B	231.7	46.5	-539.8	102.0	Over-Current
11	AFCI	12-3 NM-B	226.5	35.4	11.4	-69.9	Ground Fault
12	GFCI	12-3 NM-B	216.6	25.9	-2.1	-7.8	Ground Fault
13	MCCB	18-3 SVT	218.8	30.2	-519.5	98.7	Over-Current
14	AFCI	18-3 SVT	219.6	31.0	-513.1	96.4	Over-Current
15	GFCI	18-3 SVT	217.7	29.1	-621.0	-26.3	Over-Current
16	MCCB	18-2 NISPT-2	218.8	30.2	-427.1	-9.6	Over-Current
17	AFCI	18-2 NISPT-2	226.6	38.6	460.6	-7.4	Over-Current
18	GFCI	18-2 NISPT-2	223.7	34.7	446.1	-8.5	Over-Current

Appendix D Physical Cord Damage

Table D.1: Post Experiment Physical Observations on Cords

Circuit #	Breaker Type	Cord Type	Physical Observations						
			Exp 1	Exp 2	Exp 3	Exp 4	Exp 5	Exp 6	
1	MCCB	18-2 SPT1	Broken, beads	Broken	Broken, beads	Broken, beads	Broken	Broken	Broken
2	AFCI	18-2 SPT1	Broken	Broken strand, bead	Broken strand, beads	Broken, beads	Broken	Broken	Broken
3	GFCI	18-2 SPT1	Broken	Broken	Broken, beads	Broken, beads	Broken strands	Broken	Broken
4	MCCB	16-3 SJTW	Broken strand, beading	Broken strand, beads	Broken strand, notch	Broken strand,	—	Broken strands, beads	Broken strands
5	AFCI	16-3 SJTW	—	Bead	Broken strand	Broken strand	Broken strands	—	Notch, bead
6	GFCI	16-3 SJTW	—	Broken strand, bead	Bead	Broken strand, bead	Broken strand, bead	—	Broken strand
7	MCCB	12-2 NM-B	Notch, bead	Notch, bead	Notch, bead	Notch, bead	Notch, beads	Notch, beads	Notch, bead
8	AFCI	12-2 NM-B	—	—	—	—	—	Notch, bead	Notch
9	GFCI	12-2 NM-B	—	—	—	—	Notch	—	—
10	MCCB	12-3 NM-B	—	Notch, bead	—	—	Notch, bead	Notch, beads	—
11	AFCI	12-3 NM-B	—	—	—	—	Notches	Notch, beads	—
12	GFCI	12-3 NM-B	—	—	—	—	—	Small beads	—
13	MCCB	18-3 SVT	—	Notch, bead	—	—	—	—	Bead
14	AFCI	18-3 SVT	Broken strand	Notch, bead	Broken strands, beads	Broken strands, beads	Broken strands, beads	Broken strands	Broken strands
15	GFCI	18-3 SVT	Broken strand, beading	Bead	Broken strands	Broken strands	Broken strands	Bead	Broken strands
16	MCCB	18-2 NISPT-2	Broken strand, beading	—	Broken strands	Broken strands	Broken strands	Broken strands	Broken strands
17	AFCI	18-2 NISPT-2	Broken strand, beading	—	Broken strands	Broken strands	Broken strands	Broken strands	Broken strands
18	GFCI	18-2 NISPT-2	Broken strand, beading	Bead	Broken strands, beads	Broken strands, beads	—	Broken strands	Broken strands

— indicates no discernible damage